Effectiveness of the recursive-lattice technique in the investigation of magnetic systems with the pyrochlore structure

E. Jurčišinová and M. Jurčišin
Institute of Experimental Physics, Slovak Academy of Sciences, Watsonova 47, 040 01 Košice, Slovakia

(Received 11 December 2023; accepted 31 January 2024; published 15 February 2024)

A well-defined higher recursive approximation of the pyrochlore lattice is introduced and its relevance and effectiveness for the systematic investigation of magnetic systems with the pyrochlore structure is studied within the classical antiferromagnetic as well as ferromagnetic spin-1/2 Ising model in the presence of the external magnetic field. The exact solution of the model is found with the explicit analytic expression for the free energy per site of the lattice. The magnetization and entropy properties of all ground states of the antiferromagnetic model are determined and compared to those obtained within the lower recursive approximation of the model on the recursive tetrahedral lattice. The exact analysis of the residual entropies of the model on the introduced recursive lattice explicitly shows that the well-known Pauling entropy of the water ice cannot represent the true residual entropy of the antiferromagnetic model on the regular pyrochlore lattice in the zero external magnetic field. The improvement of the value of the critical temperature of the ferromagnetic model obtained within the introduced higher recursive approximation is also discussed. The analysis performed demonstrates the great efficiency of recursive approximations in the investigation of various magnetic systems with the pyrochlore structure, especially for frustrated antiferromagnetic systems.

DOI: 10.1103/PhysRevE.109.024114

I. INTRODUCTION

The frustrated magnetic systems belong without a doubt among the most intensively studied systems in condensed matter physics from the experimental as well as the theoretical point of view (see, e.g., Refs. [1–12] and references cited therein). This interest is primarily given by the fact that such magnetic materials exhibit various nontrivial peculiar magnetic as well as thermodynamic properties especially at low temperatures (such as the anomalous behavior of the specific heat, the presence of huge magnetocaloric effects, or the formation of various exotic states, e.g., the spin-liquid state), which are directly related to the impossibility of an unambiguous spin arrangement in such materials in the zero-temperature limit. As a result, well-defined discrete sets of ground states are formed in such magnetic systems, many of which are highly macroscopically degenerated with the presence of strict hierarchies of their residual entropies.

From a theoretical point of view, the simplest examples of the frustrated magnetic systems are pure antiferromagnetic spin-1/2 models on various regular two- or three-dimensional lattices that contain elementary cycles build up from odd numbers (usually three) of spin variables [7,9,13]. This geometric property of a regular lattice naturally prevents the possibility of an unambiguous spin arrangement of the antiferromagnetic system in the zero-temperature limit. Typical examples of such regular lattices are two-dimensional kagome, triangular, or Shastry-Sutherland lattice and the three-dimensional pyrochlore or octahedral lattice. At the same time, it is clear that the full description of the properties of real frustrated magnetic systems can be given only within the corresponding quantum models of statistical mechanics (e.g., in the framework of the Heisenberg model). However, one of the main problem that complicates the process of a systematic investigation of the properties of the two- and three-dimensional frustrated spin systems is the nonexistence of even nearly exact analytical or, at least, computational methods for analysis of such quantum systems on infinite lattices [14]. In this situation, the corresponding models of the classical statistical mechanics become very useful since, on the one hand, many typical properties of real frustrated systems can be analyzed even in the framework of the Ising and Ising-like models (e.g., the formation of highly macroscopically degenerated ground states or the anomalous behavior of the specific heat) and, on the other hand, some models can even be solved exactly [9] (e.g., as for the residual entropies of the antiferromagnetic Ising model on the kagome [15] and triangular [16] lattice) or at least analyzed within well-controlled approximation techniques. Moreover, in the last case, the systematic analysis can very often be performed even in the presence of the external magnetic field. In this respect, it is necessary to emphasize that the importance of taking into account the presence of the magnetic field when investigating magnetic systems increases significantly in the case of the frustrated magnetic systems, since the most phenomenologically interesting properties of such systems are manifested precisely in the presence of the external magnetic field (e.g., the magnetocaloric effects and associated with them phenomenologically important effective adiabatic (de)magnetization cooling processes [17–29]).

As shown by direct investigations, among very effective approximations for the investigation of classical magnetic systems belong recursive-lattice approximations (see, e.g., Refs. [12,30]). The recursive-lattice approximations are effective especially for the systematic investigation of the

geometrically frustrated magnetic systems on regular lattices, in the framework of which given regular lattice is approximated by a recursive lattice that takes into account at least basic geometric properties of the original lattice responsible for frustration [31–34]. However, the main advantage of the recursive-lattice approximations of the frustrated magnetic systems is the fact that even completely analytical exact solutions of some models can be found as, e.g., in Refs. [35–37], where even the very existence and uniqueness of the corresponding solutions of the antiferromagnetic spin-1/2 Ising model on the recursive kagome lattice and on the recursive tetrahedral lattice were proven. Moreover, the obtained magnetization properties of the models turned out to be in a complete qualitative agreement with those obtained in the framework of the Monte Carlo simulations [38,39].

However, when working with recursive-lattice approximations of magnetic systems, a natural question immediately arises, namely, whether the obtained results are stable (at least qualitatively) with respect to the possible higher recursive approximations that take into account additional information about the geometric structure of the corresponding regular lattice. A detailed analysis of this question was performed recently in Ref. [40] in the framework of the antiferromagnetic model on the kagome-like recursive lattices and it was shown that the higher recursive approximation of the kagome lattice completely preserves the expected qualitative properties of the model and, at the same time, gives numerical corrections to the results obtained in the lower recursive-lattice approximation in correct direction, i.e., towards known exact values.

The open question is whether the conclusions obtained within the recursive-lattice approximations of the models on two-dimensional kagome lattice remain valid in the framework of frustrated three-dimensional systems. This question is studied in the present paper within the antiferromagnetic spin-1/2 Ising model on the introduced so-called recursive pyrochlore lattice, which represents a natural higher recursive-lattice approximation of the model on the regular pyrochlore lattice in comparison to the basic so-called recursive tetrahedral approximation [24,37,41–45].

In this context, the present paper has several objectives. The first objective is to introduce a higher recursive-lattice approximation of the regular pyrochlore lattice that would take into account in more detail its complex geometric structure in comparison with the simple tetrahedral recursive-lattice approximation and to test its relevance and importance from the qualitative as well as the quantitative point of view.

The second nontrivial objective of the paper is to test the validity of the hypothesis stated in Ref. [40], which asserts that the values of magnetization (residual entropies) of ground states of the frustrated models obtained within a higher recursive-lattice approximation are always smaller (larger) or at most equal to those obtained within the lower approximation.

Since the Pauling residual entropy of the water ice [46] is in fact neither the real residual entropy of the water ice [47,48] nor of the antiferromagnetic Ising model on the pyrochlore lattice [38,49], the third goal of the present study is to determine potential higher recursive-lattice corrections to the Pauling residual entropy of the antiferromagnetic model in the zero external magnetic field obtained within the tetrahedral recursive-lattice approximation of the pyrochlore lattice [24]. As we will see, this residual entropy is really changed (becomes larger than the Pauling residual entropy) when the higher recursive-lattice approximation of the pyrochlore lattice is considered.

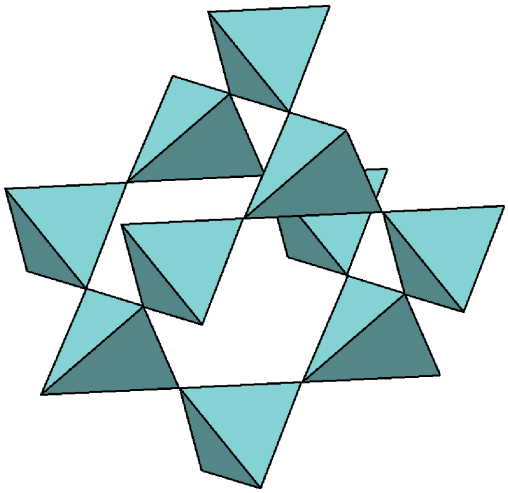

FIG. 1. Basic structure of the regular pyrochlore lattice.

The fourth objective of the present study is to determine the position of the critical temperature of the ferromagnetic model on the introduced recursive lattice and compare it to that obtained within the tetrahedral recursive-lattice approximation as well as to the critical temperatures of the model on the regular pyrochlore lattice obtained in the framework of some other approximation techniques. In this respect, let us stress that the exact position of the critical temperature of the ferromagnetic Ising model on the pyrochlore lattice is unknown.

In the end, the last but not least aim of the present study is to introduce a higher recursive-lattice approximation of the regular pyrochlore lattice in the framework of which spin models with the presence of various additional interactions could be investigated in the future, which cannot in principle be considered within the tetrahedral recursive-lattice approximation of the pyrochlore lattice.

The paper is organized as follows. In Sec. II, the model is introduced and its exact solution is present. In Sec. III, the magnetization and entropy properties of the antiferromagnetic model are investigated and all ground states of the model are determined. In Sec. IV, the ferromagnetic case of the model is studied and the value of the critical temperature is found. Finally, the obtained results are briefly reviewed and discussed in Sec. V.

II. FORMULATION OF THE MODEL

As was discussed in Introduction, our aim is to introduce a higher recursive-lattice approximation of the regular pyrochlore lattice (the basic structure of the pyrochlore lattice is shown in Fig. 1) that takes into account not only its basic tetrahedral geometric properties, as the standard tetrahedral recursive-lattice approximation does (see Fig. 2) [24,37,41–43,45], but also a typical cyclic pattern of the

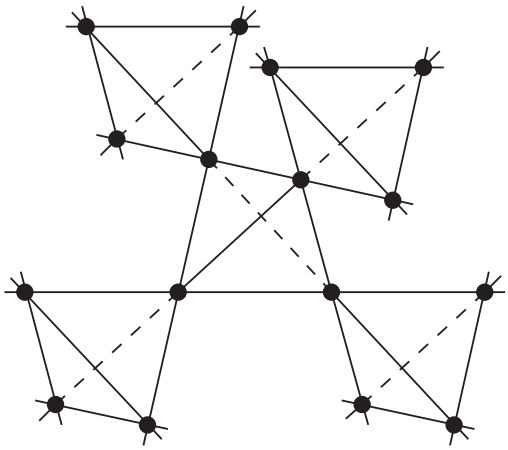

FIG. 2. Form of the recursive tetrahedral lattice with the central tetrahedron connected to the four tetrahedra of the next layer.

regular three-dimensional pyrochlore lattice formed by six connected tetrahedra (see Fig. 1, where four such cycles can be identified). The simplest recursive-lattice approximation that takes into account this property of the regular pyrochlore lattice is the recursive lattice built up recursively from elementary blocks, the explicit form of which is shown in Fig. 3.

Thus, in what follows, we will investigate in detail the spin-1/2 Ising model on the recursive lattice built up recursively from the elementary blocks shown in Fig. 3 and described by the Hamiltonian

$$\mathcal{H} = -J \sum_{\langle i\, j\rangle} s_i s_j \; - H \sum_i s_i, \tag{1}$$

where all spin variables s_i can acquire one of two possible values ± 1, J is the nearest-neighbor ferromagnetic ($J > 0$) or antiferromagnetic ($J < 0$) interaction parameter, and H denotes the external magnetic field. The first sum in Eq. (1) runs over all nearest-neighbor spin pairs and the second sum runs over over all spin sites on the studied recursive lattice.

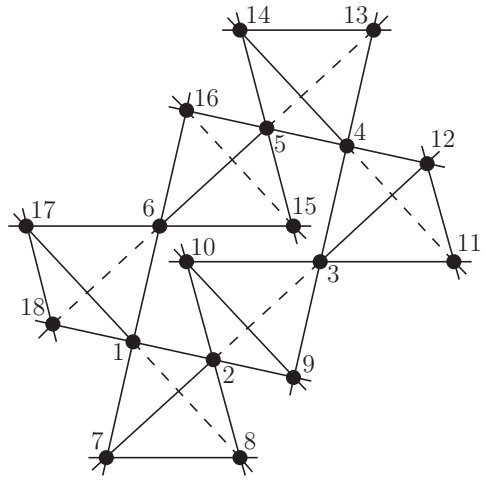

FIG. 3. Elementary block of the recursive lattice that takes into account a typical cyclic pattern of the regular pyrochlore lattice formed by six connected tetrahedra. The numbering of 18 sites of the elementary structure of the recursive lattice is used for better understanding of the partition function of the model written in Eq. (3).

Since the model described by the Hamiltonian (1) is considered on the recursive lattice, the basic geometrical structure of which is given in Fig. 3, the partition function of the studied system

$$Z \equiv \sum_s e^{-\beta \mathcal{H}} = \sum_s e^{K \sum_{\langle i\, j\rangle} s_i s_j + h \sum_i s_i}, \tag{2}$$

where the sum over s means the summation over all possible spin configurations on the lattice, $\beta = 1/(k_B T)$, T is the temperature, k_B is the Boltzmann constant, $K = \beta J$, and $h = \beta H$, can be rewritten into the following recursive form:

$$\begin{aligned} Z = \sum_{s_n^{(1)},\ldots,s_n^{(18)}} & e^{K s_n^{(1)}\left(s_n^{(2)}+s_n^{(6)}+s_n^{(7)}+s_n^{(8)}+s_n^{(17)}+s_n^{(18)}\right)} \\ & \times e^{K\left[s_n^{(2)}\left(s_n^{(3)}+s_n^{(7)}+s_n^{(8)}+s_n^{(9)}+s_n^{(10)}\right)+s_n^{(7)}s_n^{(8)}\right]} \\ & \times e^{K\left[s_n^{(3)}\left(s_n^{(4)}+s_n^{(9)}+s_n^{(10)}+s_n^{(11)}+s_n^{(12)}\right)+s_n^{(9)}s_n^{(10)}\right]} \\ & \times e^{K\left[s_n^{(4)}\left(s_n^{(5)}+s_n^{(11)}+s_n^{(12)}+s_n^{(13)}+s_n^{(14)}\right)+s_n^{(11)}s_n^{(12)}\right]} \\ & \times e^{K\left[s_n^{(5)}\left(s_n^{(6)}+s_n^{(13)}+s_n^{(14)}+s_n^{(15)}+s_n^{(16)}\right)+s_n^{(13)}s_n^{(14)}\right]} \\ & \times e^{K\left[s_n^{(6)}\left(s_n^{(15)}+s_n^{(16)}+s_n^{(17)}+s_n^{(18)}\right)+s_n^{(15)}s_n^{(16)}+s_n^{(17)}s_n^{(18)}\right]} \\ & \times e^{h\sum_{i=1}^{18} s_n^{(i)}} \prod_{j=7}^{18} u_n\left(s_n^{(j)}\right), \end{aligned} \tag{3}$$

where it is supposed that the whole recursive tree has n layers with the subsequent limit $n \to \infty$, the 18 spin variables of the central layer (the layer denoted by n) are numbered in the way shown in Fig. 3, and $u_n(s_n^{(j)})$ represent partition functions of the twelve independent branches of the whole recursive tree with base sites numbered as $j = 7, \ldots, 18$, respectively, through which they are connected to the central elementary structure built up from the six connected tetrahedra (see Fig. 3).

For completeness, let us note that since we intend to investigate the antiferromagnetic system on such a recursive "pyrochlore-like" lattice, due to the presence of geometric frustration given by four elementary triangles on each tetrahedron of the lattice, it is necessary, in general, to begin the analysis with the assumption of the existence of four different sublattices realized within each elementary tetrahedron of the lattice. However, as was proven in Ref. [37], the antiferromagnetic model on the simplest tetrahedral recursive lattice exhibits only the symmetric solutions, i.e., all sublattices of such a recursive lattice are equivalent. Although it is impossible to prove this fact in the framework of the studied higher recursive approximation of the pyrochlore lattice, nevertheless the numerical analysis shows that the same conclusion is also valid in this more complicated case. In this respect, the partition function in Eq. (3) is already written in the form when all sublattices of the whole recursive lattice are equivalent to each other.

As a result, the functions $u_n(s_n^{(i)})$ have the same form for all spin variables $s_n^{(i)})$, $i = 7, \ldots, 18$. Their values can be

calculated recursively. For instance, if the numbering of the next layer $n-1$ is performed in the same way as shown in Fig. 3, then the function $u_n(s_n^{(7)})$ is given recursively as follows:

$$u_n\big(s_n^{(7)}\big) = \sum_{s_{n-1}^{(1)},\ldots,s_{n-1}^{(6)},s_{n-1}^{(8)},\ldots,s_{n-1}^{(18)}} e^{K[s_n^{(7)}(s_{n-1}^{(1)}+s_{n-1}^{(2)}+s_{n-1}^{(8)})+s_{n-1}^{(1)}(s_{n-1}^{(2)}+s_{n-1}^{(6)}+s_{n-1}^{(8)}+s_{n-1}^{(17)}+s_{n-1}^{(18)})]}$$
$$\times e^{K[s_{n-1}^{(2)}(s_{n-1}^{(3)}+s_{n-1}^{(8)}+s_{n-1}^{(9)}+s_{n-1}^{(10)})+s_{n-1}^{(3)}(s_{n-1}^{(4)}+s_{n-1}^{(9)}+s_{n-1}^{(10)}+s_{n-1}^{(11)}+s_{n-1}^{(12)})+s_{n-1}^{(4)}(s_{n-1}^{(5)}+s_{n-1}^{(11)}+s_{n-1}^{(12)}+s_{n-1}^{(13)}+s_{n-1}^{(14)})]}$$
$$\times e^{K[s_{n-1}^{(5)}(s_{n-1}^{(6)}+s_{n-1}^{(13)}+s_{n-1}^{(14)}+s_{n-1}^{(15)}+s_{n-1}^{(16)})+s_{n-1}^{(6)}(s_{n-1}^{(15)}+s_{n-1}^{(16)}+s_{n-1}^{(17)}+s_{n-1}^{(18)})+s_{n-1}^{(9)}s_{n-1}^{(10)}+s_{n-1}^{(11)}s_{n-1}^{(12)}+s_{n-1}^{(13)}s_{n-1}^{(14)}]}$$
$$\times e^{K(s_{n-1}^{(15)}s_{n-1}^{(16)}+s_{n-1}^{(17)}s_{n-1}^{(18)})+h\sum_{i=1,i\neq 7}^{18}s_{n-1}^{(i)}}\prod_{j=8}^{18}u_{n-1}\big(s_{n-1}^{(j)}\big), \tag{4}$$

and all other functions $u_n(s_n^{(i)})$, $i=8,\ldots,18$ can be written in the similar way. Note that from a mathematical point of view all of them are completely equivalent to each other.

However, from a calculational point of view, it is more convenient to work with the only independent quantity x_n defined as the following ratio:

$$x_n = u_n(+)/u_n(-), \tag{5}$$

which can be written in the following standard recursive form:

$$x_n = \frac{\sum_{i=0}^{11} X_{1,i}x_{n-1}^i}{\sum_{i=0}^{11} X_{0,i}x_{n-1}^i}, \tag{6}$$

where the explicit form of functions $X_{1,i}$ and $X_{0,i}$ for $i=0,1,\ldots,11$ is given in Appendix A.

The fact that the studied recursive magnetic system is described by the single recursion relation (6) means that the physical properties of all possible phases of the studied model are driven by the physically relevant (real and positive) stable fixed points x of this recursion relation obtained in the limit $n\to\infty$, i.e., $x=\lim_{n\to\infty}x_n$.

Note also that all physically relevant stable fixed points of the recursion relation (6) must also belong among the solutions of the following polynomial equation of the twelfth order obtained from (6) in the limit $n\to\infty$:

$$\sum_{i=0}^{12} Y_i x^i = 0, \tag{7}$$

where the explicit form of functions Y_i, $i=0,1,\ldots,12$ is given in Appendix B.

However, knowing only the coordinates of the stable fixed points does not allow one to identify the physically relevant phase of the model in the situations when (for given values of the parameters of the model) more than one such recursively stable fixed points exist. At the same time, it is obvious that the mere knowledge of the coordinates of the physically relevant fixed points of the recursion relation (6) for given values of the parameters of the model is necessary but not sufficient condition for the description of its thermodynamics.

In this respect, the recursively stable fixed point that correspond to the thermodynamically stable phase of the model can be identified if the explicit expression for the free energy of the model is known. In addition, knowledge of the free energy of the model allows a detailed analysis of its thermodynamic properties.

The free energy per site f of the studied model can be derived using, e.g., the technique described in Ref. [50] and has the following explicit form:

$$\beta f = \frac{1}{12}\ln\left[\frac{e^{12(h+K)}F_1^5}{F_2^6}\right], \tag{8}$$

where the functions F_1 and F_2 have the following polynomial form with respect to the coordinate x of the corresponding fixed point of the recursion relation (6):

$$F_1 = \sum_{i=0}^{12} F_{1,i}x^i, \quad F_2 = \sum_{i=0}^{11} F_{2,i}x^i, \tag{9}$$

and the explicit form of all functions $F_{1,i}$ and $F_{2,i}$ is given in Appendix C.

From a theoretical point of view, the existence of the explicit expression for the free energy per site of the model as the function of the parameters of the model as well as of the coordinate x of the fixed point of the recursion relation (6) means that the present model can be considered as an exactly solvable model of the classical statistical mechanics. In what follows, we will used this exact solution for the analysis of the magnetic and entropy properties of the antiferromagnetic as well as ferromagnetic version of the model.

III. MAGNETIZATION AND ENTROPY PROPERTIES OF THE ANTIFERROMAGNETIC MODEL: RESIDUAL ENTROPIES OF ALL GROUND STATES

First, let us analyze the magnetization and entropy properties of the antiferromagnetic ($J<0$) model on the recursive lattice built from the elementary building blocks shown in Fig. 3 and compare them to those obtained within the simplest possible recursive approximation of the pyrochlore lattice, i.e., to the results of the model obtained on the tetrahedral recursive lattice (see Fig. 2). For convenience and to save space, let us call the recursive lattice built from the elementary building blocks shown in Fig. 3 as the *recursive pyrochlore lattice* (RPL) and the recursive lattice shown in Fig. 2 as the *recursive tetrahedral lattice* (RTL).

The temperature dependence of the absolute value of the total magnetization $m=-\partial f/\partial H$ and of the entropy per site $s=-\partial f/\partial T$ of the antiferromagnetic model on the RPL is

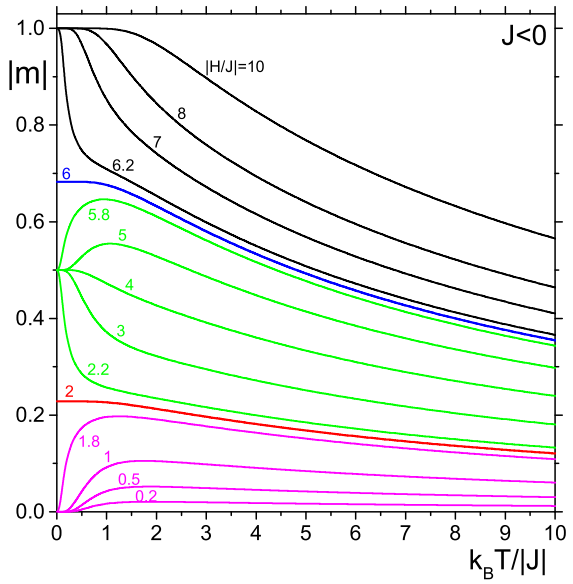

FIG. 4. Dependence of the absolute value of the total magnetization per site of the antiferromagnetic model on the RPL on the reduced temperature $k_BT/|J|$ for various absolute values of the external magnetic field $|H/J|$ with the five different ground states formed in the zero-temperature limit.

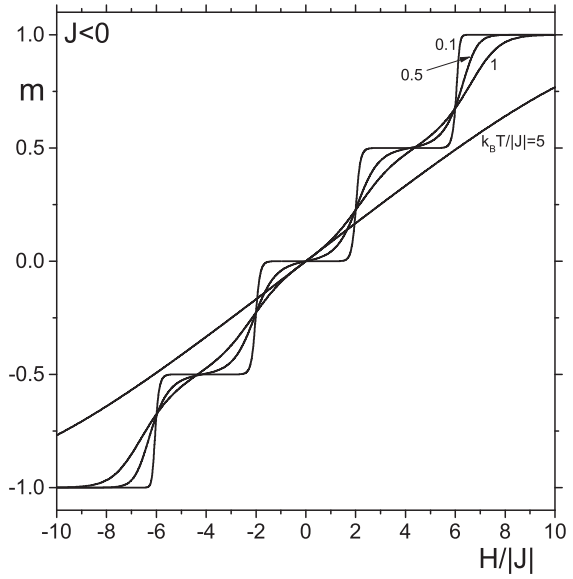

FIG. 6. Dependence of the absolute value of the total magnetization per site of the antiferromagnetic model on the RPL on the external magnetic field $H/|J|$ for various values of the reduced temperature $k_BT/|J|$.

shown in Figs. 4 and 5, respectively, for the various absolute values of the external magnetic field $|H/J|$. At the same time, the dependence of the absolute value of the total magnetization and of the entropy per site of the model on the external magnetic field $H/|J|$ for various values of the reduced temperature $k_BT/|J|$ is demonstrated in Figs. 6 and 7, respectively.

As follows from all these figures (Figs. 4–7), the model exhibits the formation of five different ground states in the zero-temperature limit with different magnetization as well as entropy properties. Three of them are the plateau ground states formed in the following intervals of the external magnetic field: the magnetization plateau with the zero magnetization ($m = 0$) is realized for $-2 < H/|J| < 2$, the second plateau ground state with $|m| = 1/2$ is formed in the

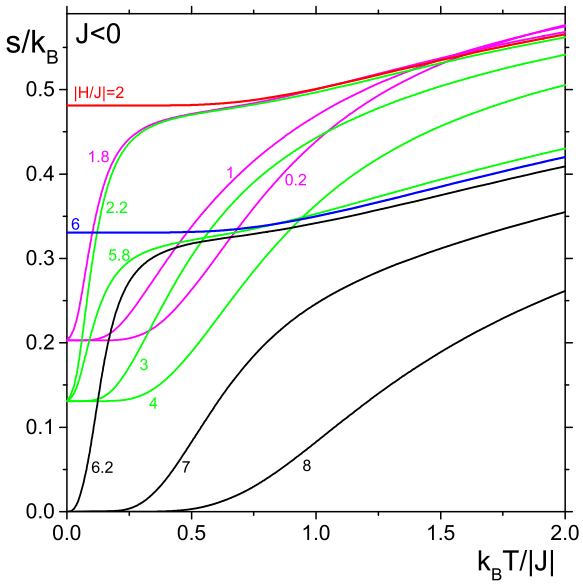

FIG. 5. Dependence of the entropy per site of the antiferromagnetic model on the RPL on the reduced temperature $k_BT/|J|$ for various absolute values of the external magnetic field $|H/J|$ with the explicit formation of nonzero residual entropies of four highly macroscopically degenerated ground states.

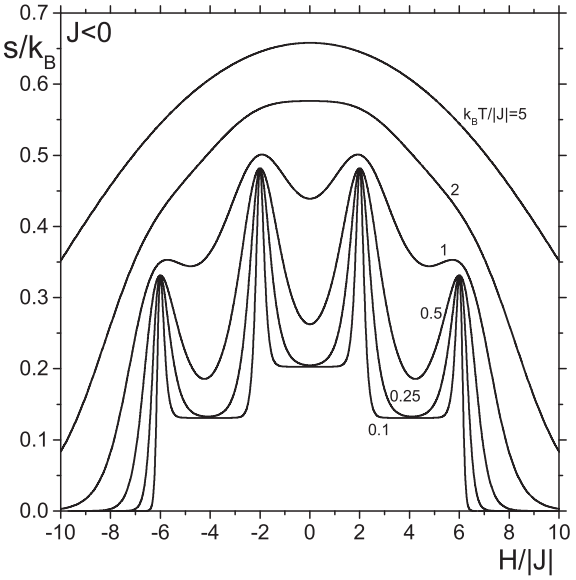

FIG. 7. Dependence of the entropy per site of the antiferromagnetic model on the RPL on the external magnetic field $H/|J|$ for various values of the reduced temperature $k_BT/|J|$ with the explicit formation of nonzero residual entropies of the highly macroscopically degenerated ground states.

interval $2 < |H/J| < 6$, and, finally, the saturated plateau ground state with $|m| = 1$ is realized for $|H/J| > 6$. Note that the same tree plateau ground states realized in the same intervals of the external magnetic field as well as with the same values of the magnetization are also formed in the case of the studied model on the RTL [37] as well as in the framework of the Monte Carlo investigations of the model on the pyrochlore lattice [38].

At the same time, as it is also clear from Figs. 4–7, the model on the RPL exhibits the formation of two single-point ground states realized at $|H/J| = 2$ and 4, respectively, which separate the aforementioned plateau ground states. The magnetization of the single-point ground states realized at $H/|J| = \pm 2$ are given as follows:

$$m = \pm \frac{m_1}{m_0}, \tag{10}$$

where

$$\begin{aligned} m_1 = x_*(&5x_*^{11} + 43x_*^{10} + 179x_*^9 + 463x_*^8 + 812x_*^7 \\ &+ 997x_*^6 + 861x_*^5 + 514x_*^4 + 209x_*^3 + 58x_*^2 \\ &+ 10x_* + 1), \end{aligned} \tag{11}$$

$$\begin{aligned} m_0 = &18x_*^{12} + 156x_*^{11} + 678x_*^{10} + 1844x_*^9 + 3423x_*^8 \\ &+ 4452x_*^7 + 4086x_*^6 + 2616x_*^5 + 1182x_*^4 + 376x_*^3 \\ &+ 84x_*^2 + 12x_* + 1, \end{aligned} \tag{12}$$

and $x_* \approx 1.261996$ is the only real positive solution of the following polynomial equation

$$\begin{aligned} &-1 - 12x_* - 71x_*^2 - 253x_*^3 - 555x_*^4 - 700x_*^5 - 371x_*^6 \\ &+ 132x_*^7 + 340x_*^8 + 236x_*^9 + 82x_*^{10} + 13x_*^{11} = 0. \end{aligned} \tag{13}$$

Their approximate numerical values are $m \approx \pm 0.228432$. Note that the absolute value of these magnetizations is only a little bit smaller than the absolute value of the corresponding magnetizations obtained in the framework of the model on the RTL ($m \approx \pm 0.228438$) [37].

However, the magnetization of the single-point ground states formed at $H/|J| = \pm 6$ are defined as follows:

$$\begin{aligned} m = \pm(&32 + 112x_* + 208x_*^2 + 232x_*^3 + 164x_*^4 + 68x_*^5 \\ &+ 13x_*^6)/(64 + 192x_* + 336x_*^2 + 352x_*^3 + 240x_*^4 \\ &+ 96x_*^5 + 18x_*^6), \end{aligned} \tag{14}$$

where now $x_* \approx 2.303006$ is the only real positive solution of the following polynomial equation

$$-16 - 56x_* - 96x_*^2 - 92x_*^3 - 44x_*^4 + 11x_*^6 + 4x_*^7 = 0. \tag{15}$$

Their approximate numerical values are $m \approx \pm 0.682667$ and their absolute value is again only a little bit smaller than the absolute value of the corresponding magnetizations obtained in the framework of the model on the RTL ($m \approx \pm 0.682679$) [37].

Thus, at least as for the magnetization properties of all the ground states of the studied antiferromagnetic model, the results obtained on the significantly more complicated RPL are very close to the corresponding results obtained in the framework of the analysis of the model within the much simpler recursive approximation of the regular pyrochlore lattice, namely, within the model on the RTL [37]. It means that, at least from the magnetization point of view, even the simplest possible recursive lattice approximation of the regular pyrochlore lattice provides quite accurate description of the antiferromagnetic spin-1/2 Ising model on the genuine pyrochlore lattice. Moreover, as will be shown and discussed a little bit later, the magnetization properties of the studied model on the RPL and on the RTL are not only very similar in the zero-temperature limit but also for arbitrary finite values of the temperature.

Now let us analyze the entropy properties of the ground states of the model on the RPL. As follows from Figs. 5 and 7, all four different nontrivial ground states of the model, i.e., all ground states except of the saturated ground states realized for $|H/J| > 6$, are highly macroscopically degenerated with strict discrete hierarchy of their nonzero residual entropies.

First, let us determine the residual entropy of the plateau ground state with zero magnetization realized in the interval $-2 < H/|J| < 2$. Its residual entropy in the framework of the studied model on the RPL is given as follows:

$$s = \frac{k_B}{12} \ln \frac{365}{32} \approx 0.202847 k_B. \tag{16}$$

This result, though very close, is different from the value of the residual entropy of this ground state of the model on the RTL [24], which is equal to the well-known Pauling entropy of the water ice ($s = k_B/2 \ln(3/2) \approx 0.202733 k_B$). In this respect, if we assume the validity of the rule that a higher approximation gives more accurate results, then the result (16) represents another evidence of the fact that the residual entropy of this ground state of the antiferromagnetic spin-1/2 Ising model on the regular pyrochlore lattice is not equal to the Pauling entropy since the higher recursive approximation of the pyrochlore lattice gives albeit small but nonzero correction to the Pauling residual entropy obtained in the framework of the model on the RTL [24]. Note that this conclusion is qualitatively in accordance with the corresponding results obtained within Monte Carlo simulations as well as other theoretical investigations (see, e.g., results and discussions in Refs. [38,49]).

The second nontrivial plateau ground state of the model realized in the interval $2 < |H/J| < 6$ with the absolute value of the magnetization $|m| = 1/2$ is also highly macroscopically degenerated (see Figs. 5 and 7) with the residual entropy given as follows:

$$s = \frac{k_B}{12} \ln \frac{2x_*^6(16 + 16x_*^2 + 3x_*^4)^6}{32 + 48x_*^2 + 18x_*^4 + x_*^6} \approx 0.130928 k_B, \tag{17}$$

where, in this case, the value of x_* is given by the only real positive solution of the equation

$$2x_*^6 + x_*^4 - 16x_*^2 - 16 = 0, \tag{18}$$

which can be written as follows:

$$x_* = \sqrt{\frac{(719 + 24\mathrm{i}\sqrt{687})^{1/3} + \frac{97}{(719+24\mathrm{i}\sqrt{687})^{1/3}} - 1}{6}}. \tag{19}$$

Its approximate numerical value is $x_* \approx 1.738536$.

TABLE I. Values of the magnetization and of the residual entropy of all ground states of the model on the recursive pyrochlore lattice (RPL) and on the recursive tetrahedral lattice (RTL) [24,37].

	$0 \leqslant \lvert H/J\rvert < 2$	$\lvert H/J\rvert = 2$	$2 < \lvert H/J\rvert < 6$	$\lvert H/J\rvert = 6$	$\lvert H/J\rvert > 6$
$\lvert m\rvert$ on the RPL	0	0.228432	0.5	0.682667	1
$\lvert m\rvert$ on the RTL	0	0.228438	0.5	0.682679	1
s/k_B on the RPL	0.202847	0.481163	0.130928	0.330681	0
s/k_B on the RTL	0.202733	0.481144	0.130812	0.330678	0

Note that the numerical value of this residual entropy is again a little bit larger than the corresponding value of the residual entropy of this plateau ground state obtained in the framework of the model on the RTL ($s \approx 0.130812 k_B$) [24].

Let us now turn to the residual entropies of two single-point ground states of the model formed at $|H/J| = 2$ and 6. The residual entropy of the first of them, i.e., of the single-point ground state realized at $|H/J| = 2$, is given as follows:

$$s = \frac{k_B}{12} \ln \frac{A^6}{B^5} \approx 0.481163 k_B, \tag{20}$$

where

$$A = 1 + 11x_* + 70x_*^2 + 282x_*^3 + 788x_*^4 + 1526x_*^5 + 2043x_*^6 + 1855x_*^7 + 1141x_*^8 + 461x_*^9 + 113x_*^{10} + 13x_*^{11}, \tag{21}$$

$$B = 1 + 12x_* + 84x_*^2 + 376x_*^3 + 1182x_*^4 + 2616x_*^5 + 4086x_*^6 + 4452x_*^7 + 3423x_*^8 + 1844x_*^9 + 678x_*^{10} + 156x_*^{11} + 18x_*^{12}, \tag{22}$$

and $x_* \approx 1.261996$ is again the only real positive solution of the polynomial equation (13). The numerical value (20) of this residual entropy is again only a little bit larger than the corresponding residual entropy obtained within the tetrahedral recursive-lattice approximation ($s \approx 0.481144 k_B$) [24].

However, the residual entropy of the single-point ground state formed at $|H/J| = 6$ in the framework of the studied pyrochlore recursive-lattice approximation is given as follows:

$$s = \frac{k_B}{12} \ln \frac{2(4x_* C)^6}{D^5} \approx 0.330681 k_B, \tag{23}$$

where

$$C = 4 + 10x_* + 14x_*^2 + 11x_*^3 + 5x_*^4 + x_*^5, \tag{24}$$

$$D = 32 + 96x_* + 168x_*^2 + 176x_*^3 + 120x_*^4 + 48x_*^5 + 9x_*^6, \tag{25}$$

and $x_* \approx 2.303006$ is the only real positive solution of the polynomial equation (15). Note that the numerical value (23) of this residual entropy is again a little bit larger than the corresponding residual entropy obtained within the tetrahedral recursive-lattice approximation ($s \approx 0.330678 k_B$) [24].

Thus, our analysis shows that (see Table I, where the magnetization and residual entropy values of all ground states of the model on the RPL are summarized and compared to those valid on the RTL) the magnetization values of all ground states of the antiferromagnetic model in the framework of the higher recursive approximation of the regular pyrochlore lattice, i.e., on the RPL with the basic structure shown in Fig. 3, are always smaller or at most equal to the corresponding values obtained in the framework of the RTL [37] (see Fig. 2), which represents the simplest possible recursive approximation of the regular pyrochlore lattice that takes into account its basic tetrahedral structure. At the same time, the residual entropies of all these ground states obtained within the higher recursive approximation are, on the contrary, always larger or at most equal to those calculated within the simpler recursive approximation [24]. This is a nontrivial fact, which is in full agreement with the corresponding hypothesis stated in Ref. [40] in the framework of the recursive investigations of the antiferromagnetic systems on the kagome lattice.

However, to be able to estimate the suitability of various recursive approximations for the systematic analysis of the magnetic and thermodynamic properties of the antiferromagnetic systems with the pyrochlore structure, it is also necessary to compare the results obtained within the pyrochlore and tetrahedral recursive-lattice approximations at nonzero temperatures.

In this respect, the effectiveness and suitability of even the simplest recursive-lattice approximation of the pyrochlore lattice given by the RTL for the systematic investigation of the corresponding antiferromagnetic systems is explicitly demonstrated in the series of Figs. 8–14, where the magnetization and entropy properties of the model on the RTL [the dashed (red) curves] and on the RPL [the solid (black) curves] as the functions of the temperature are compared for typical values of the external magnetic field $|H/J|$, namely, for $|H/J| = 2$ (Figs. 8 and 9) and $|H/J| = 6$ (Figs. 10 and 11), for which the single-point ground states are formed, and for $|H/J| = 4$ (Figs. 12 and 13) and $H = 0$ (Fig. 14) that represent typical values of the external magnetic fields, for which the plateau ground states are formed in the zero-temperature limit. Note that the magnetization of the model is always equal to zero for $H = 0$.

As follows from all these figures (Figs. 8–14), the corresponding magnetization as well as entropy curves obtained within the aforementioned two recursive approximations are almost indistinguishable. The differences can be seen only with a closer look (see the corresponding inset figures near zero temperature). At the same time, the smallness of differences $\Delta|m| = |m|_{\rm RPL} - |m|_{\rm RTL}$ and $\Delta s/k_B = (s_{\rm RPL} - s_{\rm RTL})/k_B$ between the corresponding magnetization and entropy values of the model on the RPL (values $|m|_{\rm RPL}$ and $s_{\rm RPL}/k_B$) and on the RTL (values $|m|_{\rm RTL}$ and $s_{\rm RTL}/k_B$) is also demonstrated in the corresponding inset figures in Figs. 8–14.

Finally, another important quantity, behavior of which characterizes nontrivial thermodynamic properties of the frustrated systems, is the specific heat at the constant

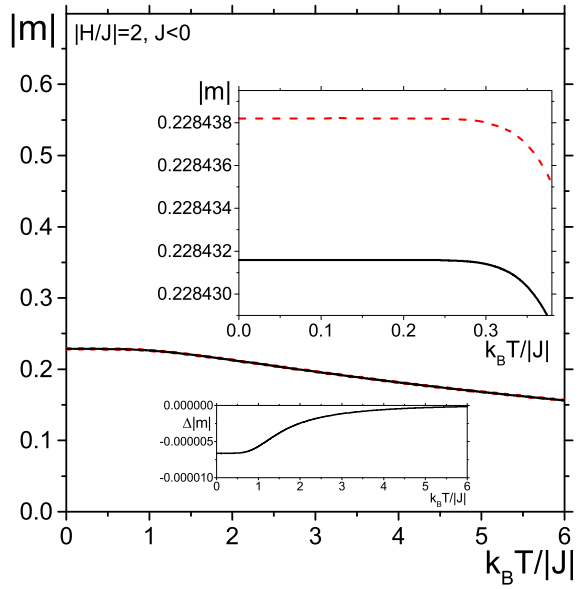

FIG. 8. The temperature dependence of the absolute value of the magnetization of the antiferromagnetic model ($J < 0$) on the RPL [the solid (black) curve] and on the RTL [the dashed (red) curve] for $|H/J| = 2$. A detailed view at low temperatures is shown in the top inset. The difference $\Delta|m|$ between these two magnetization curves is shown explicitly in the bottom inset (see the text for details).

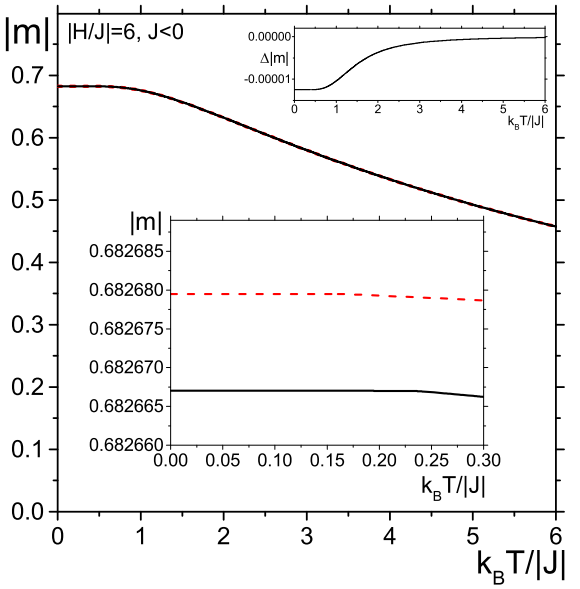

FIG. 10. Temperature dependence of the absolute value of the magnetization of the antiferromagnetic model ($J < 0$) on the RPL [the solid (black) curve] and on the RTL [the dashed (red) curve] for $|H/J| = 6$. A detailed view at low temperatures is shown in the bottom inset. The difference $\Delta|m|$ between these two magnetization curves is shown explicitly in the top inset (see the text for details).

magnetic field $c_H \equiv -T\partial^2 f/\partial T^2 = T\partial s/\partial T$. This quantity was studied in detail in Ref. [43] in the framework of the tetrahedral recursive-lattice approximation. At the same time, the adiabatic (de)magnetization cooling processes in the antiferromagnetic systems on the pyrochlore lattice were investigated in Ref. [24] in the same recursive-lattice approximation. All these results are also valid with a very high precision in the framework of the model on the RPL studied in the present paper since, as Figs. 9, 11, 13, and 14 show, there are negligible differences between the entropy properties of

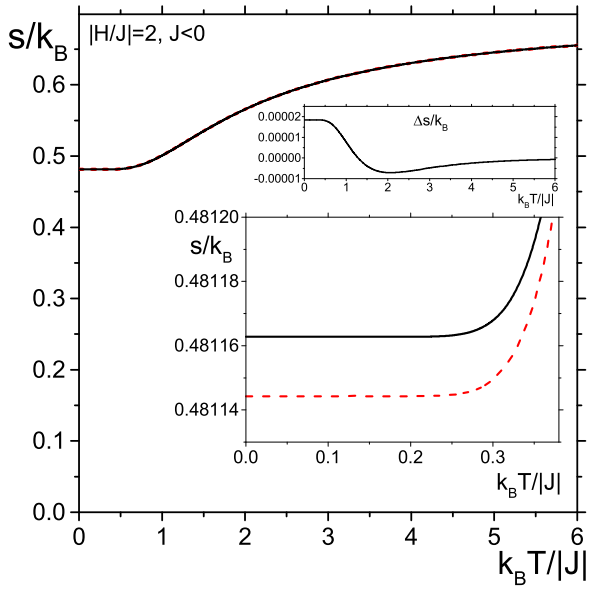

FIG. 9. Temperature dependence of the entropy per site of the antiferromagnetic model ($J < 0$) on the RPL [the solid (black) curve] and on the RTL [the dashed (red) curve] for $|H/J| = 2$. A detailed view at low temperatures is shown in the bottom inset. The difference $\Delta s/k_B$ between these two entropy curves is shown explicitly in the top inset (see the text for details).

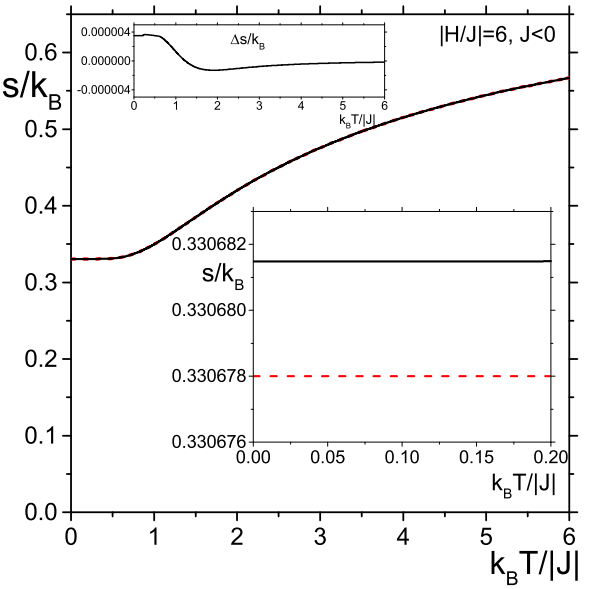

FIG. 11. Temperature dependence of the entropy per site of the antiferromagnetic model ($J < 0$) on the RPL [the solid (black) curve] and on the RTL [the dashed (red) curve] for $|H/J| = 6$. A detailed view at low temperatures is shown in the bottom inset. The difference $\Delta s/k_B$ between these two entropy curves is shown explicitly in the top inset (see the text for details).

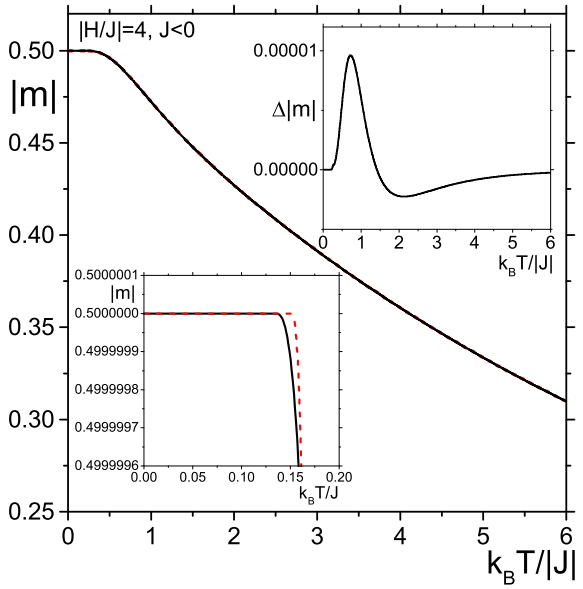

FIG. 12. Temperature dependence of the absolute value of the magnetization of the antiferromagnetic model ($J < 0$) on the RPL [the solid (black) curve] and on the RTL [the dashed (red) curve] for $|H/J| = 4$. A detailed view at low temperatures is shown in the bottom inset. The difference $\Delta|m|$ between these two magnetization curves is shown explicitly in the top inset (see the text for details).

the model on the RPL and on the RTL. Therefore, there is no need to repeat this analysis here.

Although it seems that, as the performed analysis shows, even the simpler recursive-lattice approximation given by the RTL describes appropriately the magnetic as well as

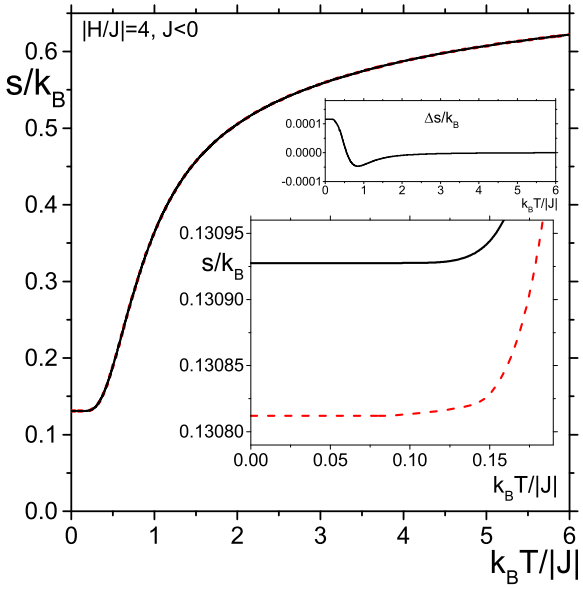

FIG. 13. Temperature dependence of the entropy per site of the antiferromagnetic model ($J < 0$) on the RPL [the solid (black) curve] and on the RTL [the dashed (red) curve] for $|H/J| = 4$. A detailed view at low temperatures is shown in the bottom inset. The difference $\Delta s/k_B$ between these two entropy curves is shown explicitly in the top inset (see the text for details).

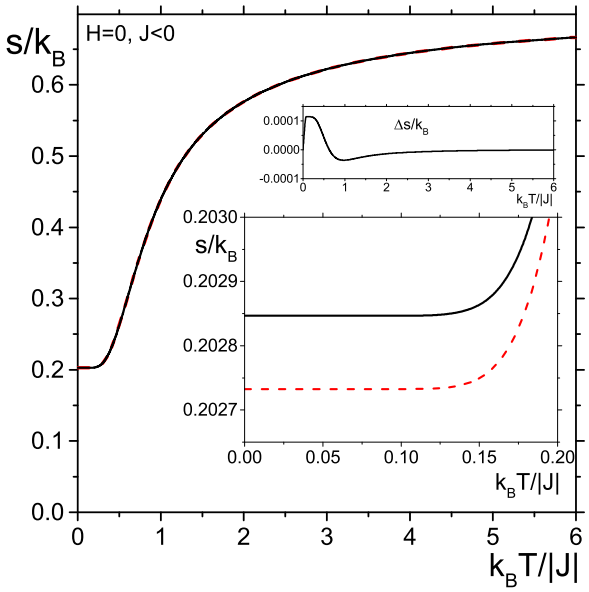

FIG. 14. Temperature dependence of the entropy per site of the antiferromagnetic model ($J < 0$) on the RPL [the solid (black) curve] and on the RTL [the dashed (red) curve] for $|H/J| = 6$. A detailed view at low temperatures is shown in the bottom inset. The difference $\Delta s/k_B$ between these two entropy curves is shown explicitly in the top inset (see the text for details).

thermodynamic properties of the geometrically frustrated antiferromagnetic systems on the regular pyrochlore lattice, nevertheless the main advantage of the introduced antiferromagnetic model on the significantly more complex RPL is that various additional interactions can be naturally added into the model on this recursive lattice with more complicated structure, which cannot in principle be taken into account in the case of the model on the RTL. For instance, among such interactions belongs the next-nearest-neighbor interaction, the presence of which can have nontrivial impact on the properties of various magnetic systems on the regular pyrochlore lattice. Thus, the introduced higher recursive-lattice approximation of the regular pyrochlore lattice opens up the possibility of studying such more complicated magnetic systems in a systematic way in the future.

IV. SPONTANEOUS MAGNETIZATION, ENTROPY, AND THE CRITICAL TEMPERATURE OF THE FERROMAGNETIC MODEL

Let us now turn our attention to the analysis of the magnetization and entropy properties of the ferromagnetic model ($J > 0$) on the RPL and compare them to those obtained on the RTL [41]. In this respect, the corresponding comparison is given in Figs. 15 and 16, respectively, for the zero external magnetic field with the explicit presence of the second order phase transition at the critical temperature. As follows from these two figures, the differences between the spontaneous magnetizations as well as between the entropies of the model on the RPL [the solid (black) lines in Figs. 15 and 16] and on RTL [the dashed (red) lines in Figs. 15 and 16] are again almost invisible (see the corresponding inset figures in Figs. 15

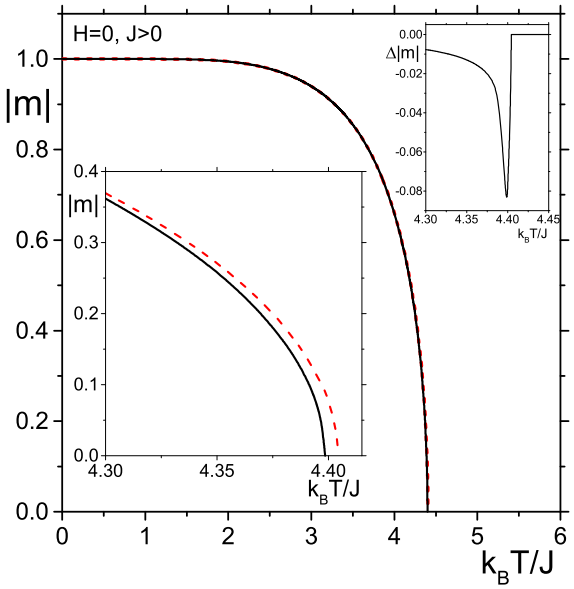

FIG. 15. The temperature dependence of the absolute value of the spontaneous magnetization of the ferromagnetic model ($J > 0$) on the RPL [the solid (black) curve] and on the RTL [the dashed (red) curve]. A detailed view in the vicinity of the corresponding critical points is shown in the bottom inset. The difference $\Delta|m|$ between these two magnetization curves is shown explicitly in the top inset (see the text for details).

and 16 that show the behavior of the magnetizations and entropies in the vicinity of the critical points of the model on the aforementioned two recursive lattices).

From a theoretical point of view, it is also both interesting and important to determine the exact position of the critical temperature of the ferromagnetic model on the studied RPL and to estimate the effectiveness of this higher recursive approximation for its determination in comparison to the known result on the RTL [41]. However, it is necessary to bear in mind that, since the Ising model on the regular pyrochlore lattice represents a three-dimensional model of the classical statistical mechanics, the exact value of the critical temperature of the Ising model on the regular pyrochlore lattice is yet unknown. At the same time, the most accurate values of the critical temperatures of three-dimensional ferromagnetic systems are usually considered to be the corresponding values obtained in the framework of series expansions. In this respect, the value of the critical temperature on the regular pyrochlore lattice was obtained, e.g., in Refs. [51,52], by using the high-temperature series expansion technique and is given as follows (in our normalization):

$$\left.\frac{k_B T_c}{J}\right|_{\mathrm{HTS}} \approx 4.21304. \tag{26}$$

However, the critical temperature of the model on the RTL was found in Ref. [41] with the numerical value (again in our normalization)

$$\left.\frac{k_B T_c}{J}\right|_{\mathrm{RTL}} \approx 4.40439, \tag{27}$$

with the relative difference $\varepsilon \approx 0.045$ with respect to the high-temperature series expansion value (26).

The value of the critical temperature $k_B T_c/J \equiv K_c^{-1}$ of the ferromagnetic model on the RPL can be found by using the same arguments as in Ref. [41] and is given by the solution of the following equation:

$$\begin{aligned}
&-440\sinh(K_c) + 346\sinh(3K_c) + 22\sinh(5K_c) - 146\sinh(7K_c) + 222\sinh(9K_c) + 398\sinh(11K_c)\\
&- 208\sinh(13K_c) + 217\sinh(15K_c) + 289\sinh(17K_c) + 94\sinh(19K_c) + 120\cosh(K_c) - 294\cosh(3K_c)\\
&+ 28\cosh(5K_c) + 156\cosh(7K_c) - 332\cosh(9K_c) - 228\cosh(11K_c) + 71\cosh(13K_c) - 142\cosh(15K_c)\\
&- 314\cosh(17K_c) - 89\cosh(19K_c) = 0.
\end{aligned} \tag{28}$$

In the end, the critical temperature $k_B T_c/J$ of the model on the RPL can be written as follows:

$$\left.\frac{k_B T_c}{J}\right|_{\mathrm{RPL}} = \frac{2}{\ln q_c} \approx 4.39848, \tag{29}$$

where $q_c > 1$ is the only such real positive solution of the following polynomial equation:

$$\begin{aligned}
&5q^{19} - 25q^{18} + 75q^{17} - 137q^{16} + 170q^{15} - 110q^{14}\\
&+ 10q^{13} + 50q^{12} + 52q^{11} - 320q^{10} + 560q^{9} - 640q^{8}\\
&+ 6q^{7} + 302q^{6} - 554q^{5} - 626q^{4} + 279q^{3} - 359q^{2}\\
&- 603q - 183 = 0.
\end{aligned} \tag{30}$$

The relative difference of this value with respect to the value of the critical temperature obtained within the high-temperature series expansion (26) is $\varepsilon \approx 0.044$, i.e., the difference between the value of the critical temperature on the RPL and the critical temperature on the regular pyrochlore lattice obtained by using the high-temperature series expansion technique is only 4.4% of the last one. Thus, the critical temperature (29) of the model on the RPL is a little bit smaller than the critical temperature (27) of the model on the RTL, i.e., the higher recursive approximation improves the value of the critical temperature toward the "exact" value (26) represented by the value obtained within the high-temperature series expansion although the improvement is small. Note that, in contrast to this small improvement of the value of the critical temperature of the ferromagnetic model on the pyrochlore lattice at the transition from the tetrahedral recursive-lattice approximation [41] to the pyrochlore recursive-lattice approximation studied in the present paper, the corresponding improvement at the transition from the Bethe recursive-lattice

TABLE II. Predictions of the value of the reduced critical temperature k_BT_c/J of the ferromagnetic spin-1/2 Ising model on the regular pyrochlore lattice in the framework of various theoretical approximations as well as by the Monte Carlo simulations (MCS) [54,55]. Namely, in the framework of the 7-site cluster effective field theory approximation (EFT) [56], the Bethe lattice approximation (BL) [53], the recursive tetrahedral lattice (RTL) [41], the recursive pyrochlore lattice (RPL) determined in the present paper, the effective field renormalization group technique (EFRG) [57], and the high-temperature series expansion [51,52], which is usually considered as the most accurate value of the critical temperature of the model on the pyrochlore lattice.

	EFT	BL	RTL	RPL	EFRG	HTSE	MCS
k_BT_c/J	4.7011	4.9326	4.40439	4.39848	4.34783	4.21304	4.21389

approximation [53] (which takes into account the value of the coordination number $z = 6$ of the regular pyrochlore lattice but no its specific geometric structure) to the tetrahedral recursive-lattice approximation [41] is quite significant since the value of the critical temperature of the model on the Bethe lattice is $k_BT_c/J = 2/\ln(3/2) \approx 4.93261$. Thus, the relative difference between this value and the value of the critical temperature (26) obtained within the high-temperature series expansion is $\varepsilon \approx 0.171$. It means that taking into account the basic tetrahedral structure of the pyrochlore lattice within the tetrahedral recursive-lattice approximation immediately almost four times improves the relative difference with respect to the value of the critical temperature obtained within the high-temperature series expansion in comparison to the Bethe lattice approximation ($\varepsilon \approx 0.045$ versus $\varepsilon \approx 0.171$). However, as our analysis shows, further significant increasing of the level of the recursive approximation of the regular pyrochlore lattice, such as the including of the basic cyclic structure of the pyrochlore lattice that consists of six connected tetrahedra, has very small impact on the value of the critical temperature. This is given by the fact that the correlation length increases to infinity at the critical temperature. Therefore the difference between the elementary geometric structures of the RTL and RPL are negligible as for the critical phenomena. However, the large difference between the critical temperatures of the model on the Bethe lattice with the coordination number $z = 6$ and on the RTL is given by the significant qualitative difference between these two recursive lattices. Namely, while the Bethe lattice with the coordination number $z = 6$ approximates not only the pyrochlore lattice but also the two-dimensional triangular lattice or the three-dimensional simple cubic lattice, the basic tetrahedral structure of the regular pyrochlore lattice is definitely fixed in the tetrahedral recursive-lattice approximation. This fact leads to the large shift of the value of the critical temperature on the RTL towards its exact value on the regular pyrochlore lattice.

For completeness, various values of the critical temperature of the ferromagnetic spin-1/2 Ising model on the pyrochlore lattice obtained in the framework of different theoretical approaches are compared in Table II.

Note also that, since, from the critical phenomena point of view, the studied ferromagnetic model on the RPL (as any model on arbitrary recursive lattice) belongs to the mean-field class of universality, all critical exponents of the model are equal to those of the mean-field theory. For instance, the exponent β that describes the asymptotic behavior of the spontaneous magnetization in the vicinity of the critical temperature at the zero external magnetic field [$m_{H=0}(T) \sim (-\tau)^{\beta}$ for $\tau = (T - T_c)/T_c$ in the limit $\tau \to 0^-$] is equal to 1/2.

Finally, let us discuss briefly the behavior of the magnetization and entropy of the ferromagnetic model on the RPL as functions of the temperature and of the external magnetic field. In this respect, the dependence of the absolute value of the magnetization on the reduced temperature k_BT/J for the various absolute values of the external magnetic field is shown explicitly in Fig. 17. However, the dependence of the magnetization on the external magnetic field H/J for various values of the reduced temperature is demonstrated in Fig. 18 with the explicit presence of the first order phase transitions at $H = 0$ below the critical temperature. In addition, the behavior of the entropy as the function of the external magnetic field for various values of the reduced temperature is shown in Fig. 19.

V. CONCLUSION

In the end, let us summarize briefly the main results obtained in the present paper.

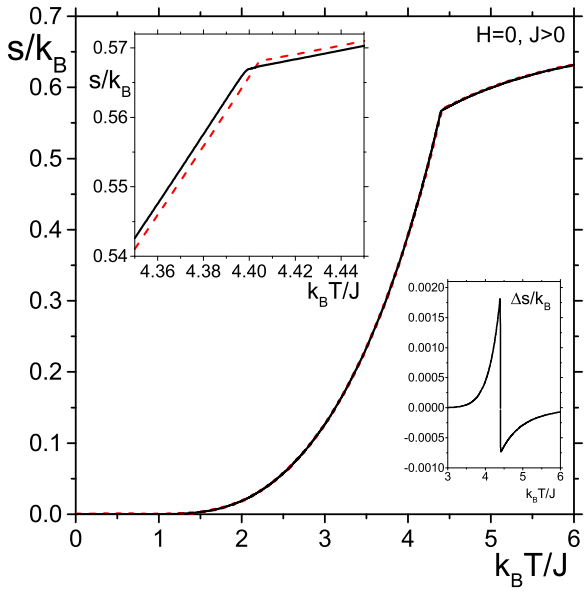

FIG. 16. The temperature dependence of the entropy per site of the ferromagnetic model ($J > 0$) on the RPL [the solid (black) curve] and on the RTL [the dashed (red) curve] for $H = 0$. A detailed view in the vicinity of the corresponding critical points is shown in the top inset. The difference $\Delta s/k_B$ between these two entropy curves is shown explicitly in the bottom inset (see the text for details).

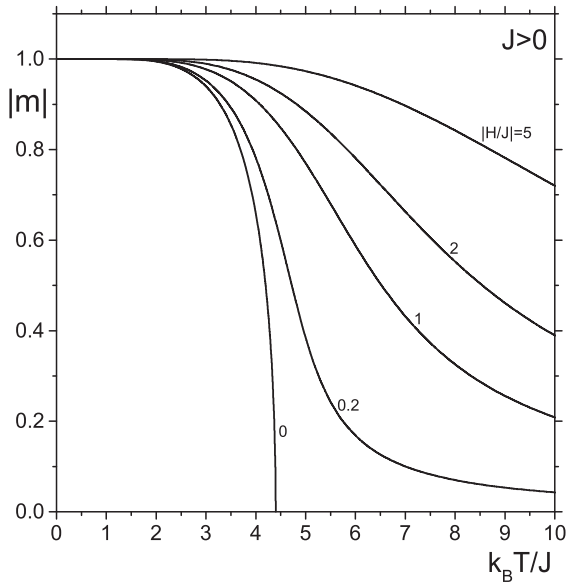

FIG. 17. The temperature dependence of the absolute value of the magnetization of the ferromagnetic model ($J > 0$) on the RPL for various absolute values of the external magnetic field.

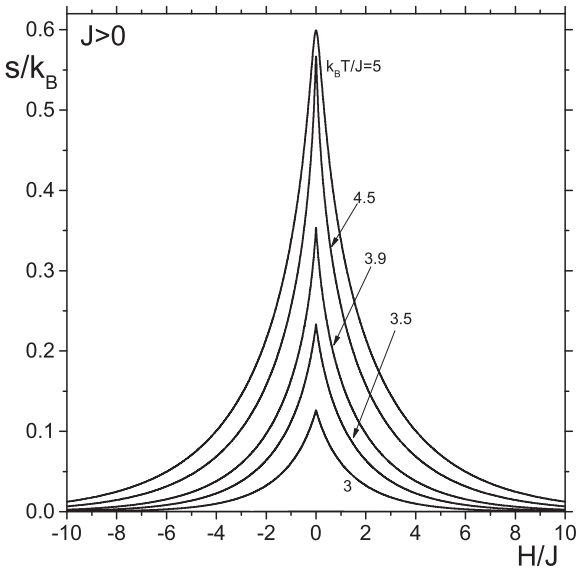

FIG. 19. Dependence of the entropy of the ferromagnetic model ($J > 0$) on the RPL on the external magnetic field for various values of the reduced temperature.

In this paper, we have introduced a higher recursive approximation of the regular pyrochlore lattice that takes into account the typical cyclic structure of the pyrochlore lattice formed by six connected elementary tetrahedra. The antiferromagnetic as well as the ferromagnetic spin-1/2 Ising models are investigated on such a recursive lattice in the presence of the external magnetic field. It is shown that such magnetic systems are exactly solvable in the sense that the explicit expression for the free energy per site of the model is found as the function of the parameters of the model and of the corresponding fixed point value of the single recursion relation, which drives all physical properties of the studied spin systems. The magnetization and entropy properties of the antiferromagnetic model are studied and it is shown that the magnetization values of all ground states are always smaller or at most equal to those obtained within the simpler approximation on the so-called recursive tetrahedral lattice. At the same time, the residual entropies of all the ground states are always larger or at most equal to the corresponding residual entropies obtained within the tetrahedral recursive-lattice approximation. These results are completely in agreement with the corresponding hypothesis states in Ref. [40] in the framework of recursive-lattice investigations of the antiferromagnetic systems on the kagome lattice. Therefore, one can conclude that the performed analysis confirms the validity of this nontrivial hypothesis in the framework of the frustrated antiferromagnetic models on the recursive lattices that approximate the regular pyrochlore lattice.

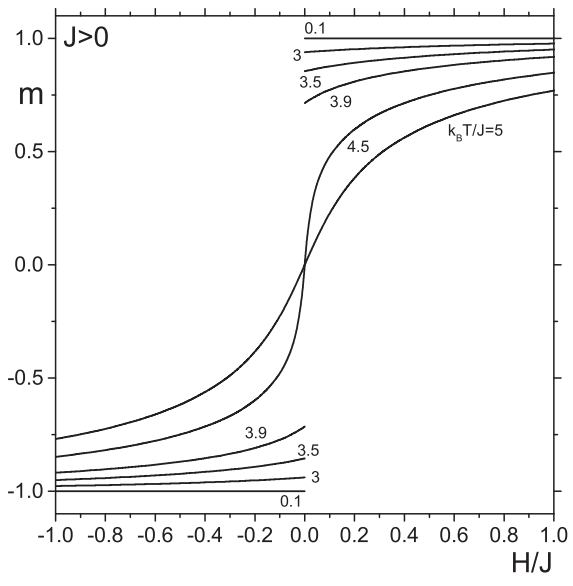

FIG. 18. Dependence of the magnetization of the ferromagnetic model ($J > 0$) on the RPL on the external magnetic field for various values of the reduced temperature with the presence of the first order phase transitions at $H = 0$ below the critical temperature.

It is also shown that the residual entropy of the highly macroscopically degenerated ground state of the antiferromagnetic model on the introduced higher recursive-lattice approximation of the regular pyrochlore lattice formed at the zero magnetic field in the zero-temperature limit is different (a little bit higher) than the Pauling residual entropy of this ground state predicted by the tetrahedral recursive-lattice approximation [24]. This fact is, on the qualitative level, in full agreement with result obtained in Ref. [49] within the investigation of the antiferromagnetic model on the pyrochlore lattice using the series expansion technique as well as with the result obtained in the framework of Monte Carlo simulations [38]. In this context, the performed analysis represents another independent confirmation of the fact that the value of the Pauling entropy does not represent the true value of the residual entropy of the antiferromagnetic Ising model on the pyrochlore lattice.

The value of critical temperature of the ferromagnetic model on the introduced RPL is determined and compare to its value obtained within the model on the RTL as well as to the corresponding values obtained in the framework of other approximative techniques.

It is also shown that the magnetization and entropy properties of the antiferromagnetic as well as the ferromagnetic Ising model on the RTL and on the introduced more complex RPL are qualitatively completely the same with very small quantitative differences. This fact demonstrates the great efficiency of the recursive-lattice approximations in the investigation of magnetic systems with the pyrochlore structure. At the same time, it is clear that the introduced higher recursive-lattice approximation allows one to include various additional interactions into the model in the future, e.g., the next-nearest-neighbor interaction, where phenomenologically interesting phenomena can be expected (see, e.g., Refs. [58,59]), or various multisite interactions, presence of which can generate frustration even in pure ferromagnetic systems [45]. We suggest that many interesting theoretical as well as important phenomenological results can still be obtained in this direction.

ACKNOWLEDGMENTS

This work was supported by the Slovak Research and Development Agency under Contract No. APVV-20-0293. This work was also supported by VEGA Grants No. 2/0044/23 and No. 2/0081/21 of the Slovak Academy of Sciences.

APPENDIX A

The explicit form of the functions $X_{0,i}$ and $X_{1,i}$ for $i = 0, 1, \ldots, 11$ in Eq. (6) is the following:

$$X_{1,0} = e^{2K}[2(e^{4K}+2)e^{2h+28K} + 2e^{10h}(2e^{4K}+1) + (5e^{4K}+3e^{8K}+7)e^{8h+4K} + 2(5e^{4K}+2e^{8K}+e^{12K}+2) \times e^{6h+8K} + (9e^{4K}+2e^{8K}+e^{12K}+3)e^{4(h+4K)} + e^{12h} + e^{40K}], \tag{A1}$$

$$X_{1,1} = e^{2h}\{(2e^{2h}+e^{4h}+10)e^{36K} + 4e^{2h+32K} + 2(5e^{2h}+e^{4h}+18)e^{2h+28K} + 3(6e^{2h}+e^{4h}+21)e^{4(h+5K)} + 2(11e^{2h}+3e^{4h}+12)e^{2h+24K} + (34e^{2h}+10e^{4h}+45)e^{8h+4K} + (70e^{2h}+24e^{4h}+e^{6h}+58)e^{6h+8K} + 3(5e^{2h}(e^{2h}+4)+21)e^{4(h+4K)} + 2[2e^{2h}(8e^{2h}+e^{4h}+19)+3]e^{4(h+3K)} + 4e^{10h} + e^{40K}\}, \tag{A2}$$

$$X_{1,2} = e^{4h+2K}\{5(3e^{4K}+8)e^{4(3h+K)} + 12(15e^{4K}+6e^{8K}+2e^{12K}+4)e^{2(h+8K)} + 6e^{10h}(28e^{4K}+12e^{8K}+6e^{12K} + 9) + 3(114e^{4K}+66e^{8K}+51e^{12K}+6e^{16K}+5e^{20K}+31)e^{4h+8K} + 3e^{8h}(119e^{4K}+62e^{8K}+45e^{12K}+13e^{16K} + 6e^{20K}+30) + 2[3e^{4K}(56e^{4K}+14e^{8K}+12e^{12K}+2e^{16K}+e^{20K}+52)+139]e^{6h+4K} + 12e^{3h+32K}\cosh h + 5e^{28K}(3e^{4K}+8)\}, \tag{A3}$$

$$X_{1,3} = e^{6h}[2(e^{2h}+1)^2e^{2h+36K} + (8e^{4h}+5)e^{32K} + 2(346e^{2h}+129e^{4h}+289)e^{6h+4K} + 6(58e^{2h}+39e^{4h}+18e^{6h} + 2e^{8h}+66)e^{2h+20K} + 2(40e^{2h}+36e^{4h}+20e^{6h}+3e^{8h}+40)e^{28K} + (128e^{2h}+90e^{4h}+80e^{6h}+27e^{8h}+80) \times e^{24K} + (1072e^{2h}+858e^{4h}+384e^{6h}+80e^{8h}+475)e^{4h+8K} + (672e^{2h}+508e^{4h}+304e^{6h}+96e^{8h}+5e^{10h} + 352)e^{2(h+8K)} + 2(403e^{2h}+393e^{4h}+212e^{6h}+120e^{8h}+40e^{10h}+16)e^{2(h+6K)} + 56e^{8h}], \tag{A4}$$

$$X_{1,4} = 5e^{8h+2K}[2(e^{2h}+1)e^{4(h+8K)} + (7e^{2h}+6e^{4h}+3e^{6h}+4)e^{2h+28K} + (454e^{2h}+361e^{4h}+116e^{6h}+217) \times e^{4(h+K)} + 2(4e^{2h}+9e^{4h}+6e^{6h}+3e^{8h}+5)e^{24K} + 2(131e^{2h}+138e^{4h}+108e^{6h}+60e^{8h}+8e^{10h}+24) \times e^{2h+8K} + (72e^{2h}+81e^{4h}+78e^{6h}+45e^{8h}+12e^{10h}+40)e^{20K} + (315e^{2h}+286e^{4h}+211e^{6h}+120e^{8h} + 40e^{10h}+172)e^{2(h+6K)} + 2(46e^{2h}+44e^{4h}+50e^{6h}+31e^{8h}+14e^{10h}+5e^{12h}+8)e^{16K} + 2e^{6h}(43e^{2h}+53)], \tag{A5}$$

$$X_{1,5} = e^{10h}\{3(e^{2h}+1)^2e^{4(h+9K)} + 12e^{6h+32K} + 3(738e^{2h}+397e^{4h}+397)e^{4(h+K)} + 12e^{6h+28K}[15\cosh(2h) + 2\cosh(4h)+9] + 12e^{6h+8K}[363\cosh(2h)+108\cosh(4h)+235] + 4e^{6(h+4K)}[81\cosh(2h)+36\cosh(4h) + 5\cosh(6h)+39] + 4e^{6(h+2K)}[867\cosh(2h)+486\cosh(4h)+16\cosh(6h)+428] + 12e^{6h+20K}[81\cosh(2h) + 54\cosh(4h)+30\cosh(6h)+58] + 12e^{6h+16K}[181\cosh(2h)+124\cosh(4h)+40\cosh(6h)+112] + 172e^{6h}\}, \tag{A6}$$

$$X_{1,6} = 7e^{2(6h+K)}\{2(e^{2h}+1)e^{6h+32K} + (6e^{2h}+7e^{4h}+4e^{6h}+3)e^{4(h+7K)} + (361e^{2h}+454e^{4h}+217e^{6h}+116) \times e^{2h+4K} + 2(6e^{2h}+9e^{4h}+4e^{6h}+5e^{8h}+3)e^{4(h+6K)} + 2(60e^{2h}+108e^{4h}+138e^{6h}+131e^{8h}+24e^{10h}+8) \times e^{8K} + (45e^{2h}+78e^{4h}+81e^{6h}+72e^{8h}+40e^{10h}+12)e^{2h+20K} + 2(14e^{2h}+31e^{4h}+50e^{6h}+44e^{8h}+46e^{10h} + 8e^{12h}+5)e^{16K} + 2e^{6h+12K}[52\sinh(2h)+26\sinh(4h)+263\cosh(2h)+146\cosh(4h)+143] + 40e^{12K} + 2e^{4h}(53e^{2h}+43)\}, \tag{A7}$$

$$X_{1,7} = 2e^{14h}(2(e^{2h}+1)^2 e^{6(h+6K)} + (5e^{4h}+8)e^{8(h+4K)} + 2(346e^{2h}+289e^{4h}+129)e^{2h+4K} + 6(18e^{2h}+39e^{4h} + 58e^{6h}+66e^{8h}+2)e^{2h+20K} + (384e^{2h}+858e^{4h}+1072e^{6h}+475e^{8h}+80)e^{8K} + 2(120e^{2h}+212e^{4h}+393e^{6h} + 403e^{8h}+16e^{10h}+40)e^{12K} + [4e^{2h}(76e^{2h}+127e^{4h}+168e^{6h}+88e^{8h}+24)+5]e^{16K} + 2e^{4(h+7K)}(20e^{2h} + 36e^{4h}+80e^{7h}\cosh h+3) + e^{4(h+6K)}\{2e^{5h}[19\sinh h + 109\cosh h + 80\cosh(3h)] + 27\} + 56e^{4h}), \tag{A8}$$

$$X_{1,8} = 3e^{2(8h+K)}[3(2e^{2h}+5e^{4h}+2)e^{8(h+4K)} + 6(3e^{2h}+12e^{4h}+2)e^{6(h+4K)} + 3(28e^{2h}+66e^{4h}+16e^{6h}+13) \times e^{4(h+4K)} + 9(8e^{2h}+17e^{4h}+20e^{6h}+2)e^{4(h+5K)} + (15e^{2h}+24e^{4h}+40e^{6h}+6)e^{6h+28K} + 3(45e^{2h}+112e^{4h} + 114e^{6h}+12)e^{2(h+6K)} + (168e^{2h}+357e^{4h}+278e^{6h}+40)e^{4K} + 3(24e^{2h}+62e^{4h}+104e^{6h}+31e^{8h}+5)e^{8K} + 18e^{2h}(5e^{2h}+3)], \tag{A9}$$

$$X_{1,9} = 5e^{18h}[(2e^{2h}+10e^{4h}+1)e^{8h+36K} + 4e^{10h+32K} + e^{12h+40K} + 2(11e^{2h}+12e^{4h}+3)e^{6(h+4K)} + 2(5e^{2h} + 18e^{4h}+1)e^{6h+28K} + 3(6e^{2h}+21e^{4h}+1)e^{4(h+5K)} + 3(20e^{2h}+21e^{4h}+5)e^{4(h+4K)} + (34e^{2h}+45e^{4h} + 10)e^{4K} + 2(16e^{2h}+38e^{4h}+3e^{6h}+2)e^{2(h+6K)} + (24e^{2h}+70e^{4h}+58e^{6h}+1)e^{8K} + 4e^{2h}], \tag{A10}$$

$$X_{1,10} = 11e^{20h+2K}[e^{2h}(e^{4K}\{e^{2h}[e^{4K}(2(e^{4K}+2)e^{6h+20K} + e^{8(h+4K)} + 2e^{2h}(5e^{4K}+2e^{8K}+e^{12K}+2) + (9e^{4K}+2e^{8K}+e^{12K}+3)e^{4h+8K} + 3e^{4K}+5) + 7] + 4\} + 2) + 1], \tag{A11}$$

$$X_{1,11} = e^{22h}(e^{4(h+4K)} + 2e^{2h+4K} + 1)\{e^{2h+4K}[e^{2h+4K}(4e^{2(h+6K)} + e^{4(h+6K)} + 6e^{4K} - e^{8K} + 1) + 4] + 1\}, \tag{A12}$$

$$X_{0,0} = (2e^{2h+4K} + e^{4h} + e^{16K})(6e^{4(h+3K)} - e^{4(h+4K)} + 4e^{6h+4K} + e^{4h+8K} + 4e^{2h+20K} + e^{8h} + e^{32K}), \tag{A13}$$

$$X_{0,1} = 11e^{2h}X_{1,0}, \quad X_{0,2} = 5e^{2h}X_{1,1}, \quad X_{0,3} = 3e^{2h}X_{1,2}, \quad X_{0,4} = 2e^{2h}X_{1,3}, \quad X_{0,5} = 7e^{2h}X_{1,4}/5,$$
$$X_{0,6} = e^{2h}X_{1,5}, \quad X_{0,7} = 5e^{2h}X_{1,6}/7, \quad X_{0,8} = e^{2h}X_{1,7}/2, \quad X_{0,9} = e^{2h}X_{1,8}/3, \quad X_{0,10} = e^{2h}X_{1,9}/5,$$
$$X_{0,11} = e^{2h}X_{1,10}/11, \tag{A14}$$

APPENDIX B

The functions Y_i for $i = 0, 1, \ldots 12$ in Eq. (7) have the following explicit form:

$$Y_0 = e^{2K}[-2(e^{4K}+2)e^{2h+28K} - 2e^{10h}(2e^{4K}+1) - (5e^{4K}+3e^{8K}+7)e^{8h+4K} - 2(5e^{4K}+2e^{8K}+e^{12K}+2) \times e^{6h+8K} - (9e^{4K}+2e^{8K}+e^{12K}+3)e^{4(h+4K)} - e^{12h} - e^{40K}], \tag{B1}$$

$$Y_1 = -(2e^{2h}+e^{4h}+4)e^{2h+36K} - 4e^{4(h+8K)} - e^{2h+40K} - 2(5e^{2h}+e^{4h}+15)e^{4(h+7K)} - 3(6e^{2h}+e^{4h}+19) \times e^{6h+20K} - (22e^{2h}+6e^{4h}+15)e^{4(h+6K)} - (34e^{2h}+10e^{4h}+39)e^{10h+4K} - (70e^{2h}+24e^{4h}+e^{6h}+49)e^{8(h+K)} - 2(35e^{2h}+16e^{4h}+2e^{6h}+2)e^{6(h+2K)} - 3[5e^{2h}(e^{2h}+4)+17]e^{6h+16K} - 3e^{12h} + e^{48K}, \tag{B2}$$

$$Y_2 = -(43e^{2h}+68)e^{2(6h+K)} + 11e^{2h+42K} - 2(9e^{2h}+6e^{4h}+25)e^{6h+26K} - (13e^{2h}+15e^{4h}+6e^{6h}-4)e^{4h+30K} - (131e^{2h}+72e^{4h}+18e^{6h}+81)e^{6h+22K} - (303e^{2h}+135e^{4h}+36e^{6h}+232)e^{8h+14K} - (154e^{2h}+84e^{4h}+39e^{6h} + 15)e^{6(h+3K)} - (313e^{2h}+168e^{4h}+40e^{6h}+201)e^{10h+6K} - (257e^{2h}+186e^{4h}+72e^{6h}+15e^{8h}+49)e^{8h+10K} + [7-6e^{2h}(e^{2h}+1)]e^{4h+34K}, \tag{B3}$$

$$Y_3 = e^{4h}[(15-8e^{4h})e^{2h+32K} - (522e^{2h}+208e^{4h}+353)e^{8h+4K} + (10e^{2h}+3e^{4h}-4e^{6h}-2e^{8h}+50)e^{36K} - 2(15e^{2h}+31e^{4h}+20e^{6h}+3e^{8h}-50)e^{2h+28K} - 3(86e^{2h}+73e^{4h}+36e^{6h}+4e^{8h}+27)e^{4(h+5K)} - (18e^{2h}+60e^{4h}+80e^{6h}+27e^{8h}-40)e^{2h+24K} - (722e^{2h}+738e^{4h}+379e^{6h}+80e^{8h}+185)e^{6h+8K} - (372e^{2h}+433e^{4h}+304e^{6h}+96e^{8h}+5e^{10h}+37)e^{4(h+4K)} - 2(213e^{2h}+313e^{4h}+202e^{6h}+120e^{8h} + 40e^{10h}+1)e^{4(h+3K)} - 36e^{10h} + 5e^{40K}], \tag{B4}$$

$$Y_4 = e^{6h+2K}\{-(1199e^{2h}+1301e^{4h}+460e^{6h}+251)e^{6h+4K} - 2(-7e^{2h}+27e^{4h}+30e^{6h}+15e^{8h}-83)e^{2h+24K} - (374e^{2h}+822e^{4h}+864e^{6h}+555e^{8h}+80e^{10h}-39)e^{4h+8K} - (567e^{2h}+1025e^{4h}+947e^{6h}+600e^{8h}+200e^{10h} - 166)e^{4(h+3K)} + [45-2e^{2h}(e^{2h}+1)(5e^{4h}-9)]e^{32K} + [340-3e^{2h}(63e^{2h}+112e^{4h}+75e^{6h}+20e^{8h}-33)] \times e^{2h+20K} + e^{28K}[120 - e^{6h}(55\sinh(2h) + 87\sinh(4h) + 5\cosh(2h) - 57\cosh(4h) + 17)] - e^{8(h+2K)} \times [122\sinh(2h) + 274\sinh(4h) + 114\sinh(6h) + 498\cosh(2h) + 6\cosh(4h) - 14\cosh(6h) + 383] - 4e^{8h}(67e^{2h}+65)\}, \tag{B5}$$

$$
\begin{aligned}
Y_5 = {} & e^{8h}\{(3e^{4h}-4)(e^{2h}+1)^2(-e^{2h+36K}) - 5(166e^{2h}+135e^{4h}+7)e^{6h+4K} - 2(-8e^{4h}+6e^{8h}-5)e^{32K} \\
& - 2(-80e^{2h}-66e^{4h}+5e^{6h}+48e^{8h}+45e^{10h}+6e^{12h}-80)e^{28K} - 6(-62e^{2h}+3e^{4h}+80e^{6h}+77e^{8h}+54e^{10h} \\
& + 30e^{12h}-102)e^{2h+20K} - 2e^{24K}(e^{2h}\{-54e^{2h}+2e^{8h}[-19\sinh h + 4\sinh(3h) + 81\cosh h + 6\cosh(3h)]\cosh h \\
& - 123\} - 80) - 2e^{8(h+K)}[688\sinh(2h) + 395\sinh(4h) + 722\cosh(2h) + 93\cosh(4h) + 552] - 4e^{8h+12K} \\
& \times [273\sinh(2h) + 363\sinh(4h) + 16\sinh(6h) + 354\cosh(2h) + 43\cosh(4h) + 216] - 2e^{8(h+2K)} \\
& \times [412\sinh(2h) + 667\sinh(4h) + 352\sinh(6h) + 482\cosh(2h) + 67\cosh(4h) - 112\cosh(6h) + 368] - 60e^{8h}\}, \qquad \text{(B6)} \\
Y_6 = {} & 14e^{17h+2K}(-e^{4K}\{e^{4K}[3e^{4K}(20e^{4K}+23e^{8K}+6e^{12K}+65)+142]+101\}\sinh(3h) \\
& - 2e^{8K}(e^{4K}\{e^{4K}[4e^{4K}(e^{4K}+9)+41]+66\}+16)\sinh(5h) - 2e^{16K}[5e^{4K}(e^{4K}+4)+8]\sinh(7h) \\
& - \sinh h\{4e^{28K}\cosh^2 h[8\cosh(2h)+2e^{4K}+3] + 93e^{4K} + 60e^{8K} + 75e^{12K} + 38e^{16K} + 33e^{20K} + 6e^{24K} + 20\}), \qquad \text{(B7)} \\
Y_7 = {} & e^{12h}(-(4e^{4h}-3)(e^{2h}+1)^2e^{4(h+9K)} + 5(166e^{2h}+7e^{4h}+135)e^{4(h+K)} - 2(8e^{4h}+5e^{8h}-6)e^{6h+32K} \\
& - 2(-705e^{2h}-552e^{4h}-17e^{6h}+151e^{8h}-244)e^{2h+8K} - 2(-367e^{2h}-447e^{4h}-368e^{6h}-35e^{8h}+300e^{10h} \\
& + 232e^{12h}-120)e^{16K} - 2e^{2h+28K}\{e^{7h}[71\sinh h + 128\sinh(3h) + 125\sinh(5h) + 61\cosh(h) + 32\cosh(3h) \\
& + 35\cosh(5h)] - 6\} + 4e^{6(h+2K)}[-273\sinh(2h) - 363\sinh(4h) - 16\sinh(6h) + 354\cosh(2h) + 43\cosh(4h) + 216] \\
& - 12e^{6h+20K}[37\sinh(2h) + 58\sinh(4h) + 66\sinh(6h) - 40\cosh(2h) + 4\cosh(4h) + 36\cosh(6h) - 40] - 2e^{24K} \\
& \times \{e^{8h}[105\sinh(2h) + 204\sinh(4h) + 116\sinh(6h) + 3\cosh(2h) + 42\cosh(4h) + 44\cosh(6h) - 1] - 5\} + 60e^{6h}), \\
& \qquad \text{(B8)} \\
Y_8 = {} & e^{2(7h+K)}[(1301e^{2h}+1199e^{4h}+251e^{6h}+460)e^{2h+4K} - 2(-30e^{2h}-27e^{4h}+7e^{6h}+83e^{8h}-15)e^{4(h+6K)} \\
& + (225e^{2h}+336e^{4h}+189e^{6h}-99e^{8h}-340e^{10h}+60)e^{2h+20K} + (600e^{2h}+947e^{4h}+1025e^{6h}+567e^{8h}-166e^{10h} \\
& + 200)e^{12K} + (555e^{2h}+864e^{4h}+822e^{6h}+374e^{8h}-39e^{10h}+80)e^{8K} + (140e^{2h}+310e^{4h}+383e^{6h}+188e^{8h} \\
& - 134e^{10h} - 64e^{12h} + 50)e^{16K} + e^{6h+32K}[5(2e^{2h}-9e^{8h}+2) - 36e^{5h}\cosh h] + e^{4(h+7K)} \\
& \times \{15 - e^{6h}[89\sinh(2h) + 150\sinh(4h) + 55\cosh(2h) + 90\cosh(4h) + 25]\} + 4e^{4h}(65e^{2h}+67)], \qquad \text{(B9)} \\
Y_9 = {} & e^{16h}[(8-15e^{4h})e^{8(h+4K)} - 5e^{14h+40K} + (522e^{2h}+353e^{4h}+208)e^{2h+4K} + (4e^{2h}-3e^{4h}-10e^{6h}-50e^{8h}+2) \\
& \times e^{6(h+6K)} + (80e^{2h}+60e^{4h}+18e^{6h}-40e^{8h}+27)e^{4(h+6K)} + 3(36e^{2h}+73e^{4h}+86e^{6h}+27e^{8h}+4)e^{2h+20K} \\
& - 2(-20e^{2h}-31e^{4h}-15e^{6h}+50e^{8h}-3)e^{4(h+7K)} + (379e^{2h}+738e^{4h}+722e^{6h}+185e^{8h}+80)e^{8K} \\
& + 2(120e^{2h}+202e^{4h}+313e^{6h}+213e^{8h}+e^{10h}+40)e^{12K} + (96e^{2h}+304e^{4h}+433e^{6h}+372e^{8h}+37e^{10h}+5) \\
& \times e^{16K} + 36e^{4h}], \qquad \text{(B10)} \\
Y_{10} = {} & e^{2(9h+K)}[-11e^{14h+40K} + (6e^{2h}-7e^{4h}+6)e^{8(h+4K)} + 2(9e^{2h}+25e^{4h}+6)e^{6(h+4K)} + (15e^{2h}+13e^{4h} \\
& - 4e^{6h}+6)e^{6h+28K} + (84e^{2h}+154e^{4h}+15e^{6h}+39)e^{4(h+4K)} + (72e^{2h}+131e^{4h}+81e^{6h}+18)e^{4(h+5K)} \\
& + (168e^{2h}+313e^{4h}+201e^{6h}+40)e^{4K} + (135e^{2h}+303e^{4h}+232e^{6h}+36)e^{2(h+6K)} + (72e^{2h}+186e^{4h} \\
& + 257e^{6h}+49e^{8h}+15)e^{8K} + e^{2h}(68e^{2h}+43)], \qquad \text{(B11)} \\
Y_{11} = {} & e^{20h}[(2e^{2h}+4e^{4h}+1)e^{8h+36K} + 4e^{10h+32K} + e^{12h+40K} - e^{14h+48K} + 2(5e^{2h}+15e^{4h}+1)e^{6h+28K} \\
& + (22e^{2h}+15e^{4h}+6)e^{6(h+4K)} + 3(20e^{2h}+17e^{4h}+5)e^{4(h+4K)} + 3(6e^{2h}+19e^{4h}+1)e^{4(h+5K)} + (34e^{2h} \\
& + 39e^{4h}+10)e^{4K} + 2(16e^{2h}+35e^{4h}+2e^{6h}+2)e^{2(h+6K)} + (24e^{2h}+70e^{4h}+49e^{6h}+1)e^{8K} + 3e^{2h}], \qquad \text{(B12)} \\
Y_{12} = {} & e^{22h+2K}(7e^{4(h+K)} + 10e^{6(h+2K)} + 3e^{8(h+2K)} + 3e^{4(h+3K)} + 2e^{8(h+3K)} + 4e^{2h+4K} + 5e^{4h+8K} + 4e^{6h+8K} \\
& + 4e^{6h+16K} + 2e^{6h+20K} + 9e^{8h+20K} + e^{8h+28K} + 4e^{10h+28K} + 2e^{10h+32K} + e^{12h+40K} + 2e^{2h} + 1). \qquad \text{(B13)}
\end{aligned}
$$

APPENDIX C

The explicit form of the functions $F_{1,i}$ and $F_{2,i}$ in Eq. (9) is the following:

$$
\begin{aligned}
F_{1,0} = {} & (2e^{2h+4K} + e^{4h} + e^{16K})(6e^{4(h+3K)} - e^{4(h+4K)} + 4e^{6h+4K} + e^{4h+8K} + 4e^{2h+20K} + e^{8h} + e^{32K}), \qquad \text{(C1)} \\
F_{1,1} = {} & 12e^{2(h+K)}[2(e^{4K}+2)e^{2h+28K} + 2e^{10h}(2e^{4K}+1) + (5e^{4K}+3e^{8K}+7)e^{8h+4K} \\
& + 2(5e^{4K}+2e^{8K}+e^{12K}+2)e^{6h+8K} + (9e^{4K}+2e^{8K}+e^{12K}+3)e^{4(h+4K)} + e^{12h} + e^{40K}], \qquad \text{(C2)}
\end{aligned}
$$

$$F_{1,2} = 6e^{4h}\{(2e^{2h} + e^{4h} + 10)e^{36K} + 4e^{2h+32K} + 2(5e^{2h} + e^{4h} + 18)e^{2h+28K} + 3(6e^{2h} + e^{4h} + 21)e^{4(h+5K)} + 2(11e^{2h} + 3e^{4h} + 12)e^{2h+24K} + (34e^{2h} + 10e^{4h} + 45)e^{8h+4K} + (70e^{2h} + 24e^{4h} + e^{6h} + 58)e^{6h+8K} + 3[5e^{2h}(e^{2h} + 4) + 21]e^{4(h+4K)} + 2[2e^{2h}(8e^{2h} + e^{4h} + 19) + 3]e^{4(h+3K)} + 4e^{10h} + e^{40K}\}, \quad \text{(C3)}$$

$$F_{1,3} = 4e^{6h+2K}\{5(3e^{4K} + 8)e^{4(3h+K)} + 12(15e^{4K} + 6e^{8K} + 2e^{12K} + 4)e^{2(h+8K)} + 6e^{10h}(28e^{4K} + 12e^{8K} + 6e^{12K} + 9) + 3(114e^{4K} + 66e^{8K} + 51e^{12K} + 6e^{16K} + 5e^{20K} + 31)e^{4h+8K} + 3e^{8h}(119e^{4K} + 62e^{8K} + 45e^{12K} + 13e^{16K} + 6e^{20K} + 30) + 2[3e^{4K}(56e^{4K} + 14e^{8K} + 12e^{12K} + 2e^{16K} + e^{20K} + 52) + 139]e^{6h+4K} + 12e^{3h+32K}\cosh h + 5e^{28K}(3e^{4K} + 8)\}, \quad \text{(C4)}$$

$$F_{1,4} = 3e^{8h}[2(e^{2h} + 1)^2 e^{2h+36K} + (8e^{4h} + 5)e^{32K} + 2(346e^{2h} + 129e^{4h} + 289)e^{6h+4K} + 6(58e^{2h} + 39e^{4h} + 18e^{6h} + 2e^{8h} + 66)e^{2h+20K} + 2(40e^{2h} + 36e^{4h} + 20e^{6h} + 3e^{8h} + 40)e^{28K} + (128e^{2h} + 90e^{4h} + 80e^{6h} + 27e^{8h} + 80) \times e^{24K} + (1072e^{2h} + 858e^{4h} + 384e^{6h} + 80e^{8h} + 475)e^{4h+8K} + (672e^{2h} + 508e^{4h} + 304e^{6h} + 96e^{8h} + 5e^{10h} + 352)e^{2(h+8K)} + 2(403e^{2h} + 393e^{4h} + 212e^{6h} + 120e^{8h} + 40e^{10h} + 16)e^{2(h+6K)} + 56e^{8h}], \quad \text{(C5)}$$

$$F_{1,5} = 12e^{2(5h+K)}[2(e^{2h} + 1)e^{4(h+8K)} + (7e^{2h} + 6e^{4h} + 3e^{6h} + 4)e^{2h+28K} + (454e^{2h} + 361e^{4h} + 116e^{6h} + 217) \times e^{4(h+K)} + 2(4e^{2h} + 9e^{4h} + 6e^{6h} + 3e^{8h} + 5)e^{24K} + 2(131e^{2h} + 138e^{4h} + 108e^{6h} + 60e^{8h} + 8e^{10h} + 24) \times e^{2h+8K} + (72e^{2h} + 81e^{4h} + 78e^{6h} + 45e^{8h} + 12e^{10h} + 40)e^{20K} + (315e^{2h} + 286e^{4h} + 211e^{6h} + 120e^{8h} + 40e^{10h} + 172)e^{2(h+6K)} + 2(46e^{2h} + 44e^{4h} + 50e^{6h} + 31e^{8h} + 14e^{10h} + 5e^{12h} + 8)e^{16K} + 2e^{6h}(43e^{2h} + 53)], \quad \text{(C6)}$$

$$F_{1,6} = 2e^{12h}\{3(e^{2h} + 1)^2 e^{4(h+9K)} + 12e^{6h+32K} + 3(738e^{2h} + 397e^{4h} + 397)e^{4(h+K)} + 12e^{6h+28K}[15\cosh(2h) + 2\cosh(4h) + 9] + 12e^{6h+8K}[363\cosh(2h) + 108\cosh(4h) + 235] + 4e^{6(h+4K)}[81\cosh(2h) + 36\cosh(4h) + 5\cosh(6h) + 39] + 4e^{6(h+2K)}[867\cosh(2h) + 486\cosh(4h) + 16\cosh(6h) + 428] + 12e^{6h+20K}[81\cosh(2h) + 54\cosh(4h) + 30\cosh(6h) + 58] + 12e^{6h+16K}[181\cosh(2h) + 124\cosh(4h) + 40\cosh(6h) + 112] + 172e^{6h}\}, \quad \text{(C7)}$$

$$F_{1,7} = 12e^{2(7h+K)}\{2(e^{2h} + 1)e^{6h+32K} + (6e^{2h} + 7e^{4h} + 4e^{6h} + 3)e^{4(h+7K)} + (361e^{2h} + 454e^{4h} + 217e^{6h} + 116) \times e^{2h+4K} + 2(6e^{2h} + 9e^{4h} + 4e^{6h} + 5e^{8h} + 3)e^{4(h+6K)} + 2(60e^{2h} + 108e^{4h} + 138e^{6h} + 131e^{8h} + 24e^{10h} + 8) \times e^{8K} + (45e^{2h} + 78e^{4h} + 81e^{6h} + 72e^{8h} + 40e^{10h} + 12)e^{2h+20K} + 2(14e^{2h} + 31e^{4h} + 50e^{6h} + 44e^{8h} + 46e^{10h} + 8e^{12h} + 5)e^{16K} + 2e^{6h+12K}[52\sinh(2h) + 26\sinh(4h) + 263\cosh(2h) + 146\cosh(4h) + 143] + 40e^{12K} + 2e^{4h}(53e^{2h} + 43)\}, \quad \text{(C8)}$$

$$F_{1,8} = 3e^{16h}\{2(e^{2h} + 1)^2 e^{6(h+6K)} + (5e^{4h} + 8)e^{8(h+4K)} + 2(346e^{2h} + 289e^{4h} + 129)e^{2h+4K} + 6(18e^{2h} + 39e^{4h} + 58e^{6h} + 66e^{8h} + 2)e^{2h+20K} + (384e^{2h} + 858e^{4h} + 1072e^{6h} + 475e^{8h} + 80)e^{8K} + 2(120e^{2h} + 212e^{4h} + 393e^{6h} + 403e^{8h} + 16e^{10h} + 40)e^{12K} + (4e^{2h}(76e^{2h} + 127e^{4h} + 168e^{6h} + 88e^{8h} + 24) + 5)e^{16K} + 2e^{4(h+7K)}(20e^{2h} + 36e^{4h} + 80e^{7h}\cosh h + 3) + 2e^{9h+24K}[19\sinh h + 109\cosh h + 80\cosh(3h)] + 27e^{4(h+6K)} + 56e^{4h}\}, \quad \text{(C9)}$$

$$F_{1,9} = 4e^{2(9h+K)}[3(2e^{2h} + 5e^{4h} + 2)e^{8(h+4K)} + 6(3e^{2h} + 12e^{4h} + 2)e^{6(h+4K)} + 3(28e^{2h} + 66e^{4h} + 16e^{6h} + 13) \times e^{4(h+4K)} + 9(8e^{2h} + 17e^{4h} + 20e^{6h} + 2)e^{4(h+5K)} + (15e^{2h} + 24e^{4h} + 40e^{6h} + 6)e^{6h+28K} + 3(45e^{2h} + 112e^{4h} + 114e^{6h} + 12)e^{2(h+6K)} + (168e^{2h} + 357e^{4h} + 278e^{6h} + 40)e^{4K} + 3(24e^{2h} + 62e^{4h} + 104e^{6h} + 31e^{8h} + 5)e^{8K} + 18e^{2h}(5e^{2h} + 3)], \quad \text{(C10)}$$

$$F_{1,10} = 6e^{20h}[(2e^{2h} + 10e^{4h} + 1)e^{8h+36K} + 4e^{10h+32K} + e^{12h+40K} + 2(11e^{2h} + 12e^{4h} + 3)e^{6(h+4K)} + 2(5e^{2h} + 18e^{4h} + 1)e^{6h+28K} + 3(6e^{2h} + 21e^{4h} + 1)e^{4(h+5K)} + 3(20e^{2h} + 21e^{4h} + 5)e^{4(h+4K)} + (34e^{2h} + 45e^{4h} + 10)e^{4K} + 2(16e^{2h} + 38e^{4h} + 3e^{6h} + 2)e^{2(h+6K)} + (24e^{2h} + 70e^{4h} + 58e^{6h} + 1)e^{8K} + 4e^{2h}], \quad \text{(C11)}$$

$$F_{1,11} = 12e^{22h+2K}(7e^{4(h+K)} + 10e^{6(h+2K)} + 3e^{8(h+2K)} + 3e^{4(h+3K)} + 2e^{8(h+3K)} + 4e^{2h+4K} + 5e^{4h+8K} + 4e^{6h+8K} + 4e^{6h+16K} + 2e^{6h+20K} + 9e^{8h+20K} + e^{8h+28K} + 4e^{10h+28K} + 2e^{10h+32K} + e^{12h+40K} + 2e^{2h} + 1), \quad \text{(C12)}$$

$$F_{1,12} = e^{24h}(2e^{6(h+2K)} + 6e^{4(h+3K)} + 9e^{8(h+3K)} + e^{12(h+4K)} + 6e^{2h+4K} + 9e^{4h+8K} + 12e^{6h+16K} + 6e^{6h+20K} + 6e^{8h+28K} + 6e^{10h+36K} + 1), \quad \text{(C13)}$$

$$F_{2,0} = F_{1,0}, \quad F_{2,1} = 11F_{1,1}/12, \quad F_{2,2} = 5F_{1,2}/6, \quad F_{2,3} = 3F_{1,3}/4, \quad F_{2,4} = 2F_{1,4}/3, \tag{C14}$$

$$F_{2,5} = 7F_{1,5}/12, \quad F_{2,6} = F_{1,6}/2, \quad F_{2,7} = 5F_{1,7}/12, \quad F_{2,8} = F_{1,8}/3, \quad F_{2,9} = F_{1,9}/4, \tag{C15}$$

$$F_{2,10} = F_{1,10}/6, \quad F_{2,11} = F_{1,11}/12. \tag{C16}$$

[1] D. Chowdhury, *Spin Glasses and Other Frustrated Systems* (World Scientific, Singapore, 1986).
[2] A. P. Ramirez, Annu. Rev. Mater. Sci. **24**, 453 (1994).
[3] J. E. Greedan, J. Mater. Chem. **11**, 37 (2001).
[4] R. Moessner, Can. J. Phys. **79**, 1283 (2001).
[5] J. Richter, J. Schulenburg, and A. Honecker, Quantum magnetism in two dimensions: From semi-classical Néel order to magnetic disorder, Quantum Magnetism, Lect. Notes Phys. **645**, 85 (2004).
[6] L. Balents, Nature (London) **464**, 199 (2010).
[7] J. S. Gardner, M. J. P. Gingras, and J. E. Greedan, Rev. Mod. Phys. **82**, 53 (2010).
[8] C. Lacroix, P. Mendels, and F. Mila (eds.), *Introduction to Frustrated Magnetism*, Springer Series in Solid-State Sciences 164 (Springer-Verlag, Berlin, 2011).
[9] H. T. Diep (Ed.), *Frustrated Spin Systems* (World Scientific, Singapore, 2013).
[10] T. Lookman and X. Ren (eds.), *Frustrated Materials and Ferroic Glasses* (Springer Nature, Switzerland, 2018).
[11] L. Savary and L. Balents, Rep. Prog. Phys. **80**, 016502 (2017).
[12] J. L. Monroe, Phys. Rev. E **64**, 016126 (2001).
[13] G. Toulouse, Commun. Phys. **2**, 115 (1977).
[14] S. Yan, D. A. Huse, and S. R. White, Science **332**, 1173 (2011).
[15] K. Kanô and S. Naya, Prog. Theor. Phys. **10**, 158 (1953).
[16] G. H. Wannier, Phys. Rev. **79**, 357 (1950).
[17] A. P. Ramirez, A. Hayashi, R. J. Cava, R. Siddharthan, and B. S. Shastry, Nature (London) **399**, 333 (1999).
[18] K. Matsuhira, Z. Hiroi, T. Tayama, S. Takagi, and T. Sakakibara, J. Phys.: Condens. Matter **14**, L559 (2002).
[19] Z. Hiroi, K. Matsuhira, S. Takagi, T. Tayama, and T. Sakakibara, J. Phys. Soc. Jpn. **72**, 411 (2003).
[20] S. S. Sosin, L. A. Prozorova, A. I. Smirnov, A. I. Golov, I. B. Berkutov, O. A. Petrenko, G. Balakrishnan, and M. E. Zhitomirsky, Phys. Rev. B **71**, 094413 (2005).
[21] X. Ke, D. V. West, R. J. Cava, and P. Schiffer, Phys. Rev. B **80**, 144426 (2009).
[22] A. M. Hallas, A. M. Arevalo-Lopez, A. Z. Sharma, T. Munsie, J. P. Attfield, C. R. Wiebe, and G. M. Luke, Phys. Rev. B **91**, 104417 (2015).
[23] B. Wolf, U. Tutsch, S. Dörschung, C. Krellner, F. Ritter, W. Assmus, and M. Lang, J. Appl. Phys. **120**, 142112 (2016).
[24] E. Jurčišinová and M. Jurčišin, Phys. Rev. E **96**, 052128 (2017).
[25] S. Lucas, K. Grube, C.-L. Huang, A. Sakai, S. Wunderlich, E. L. Green, J. Wosnitza, V. Fritsch, P. Gegenwart, O. Stockert, and H. v. LÖhneysen, Phys. Rev. Lett. **118**, 107204 (2017).
[26] Y. Tokiwa, S. Bachus, K. Kavita, A. Jesche, A. A. Tsirlin, and P. Gegenwart, Commun. Mater. **2**, 42 (2020).
[27] N. Terada and H. Mamyia, Nat. Commun. **12**, 1212 (2021).
[28] X. Tang, A. Sepehri-Amin, N. Terada, A. Martin-Cid, I. Kurniawan, S. Kobayashi, Y. Kotani, H. Takeya, J. Lai, Y. Matsushita, T. Ohkubo, Y. Miura, T. Nakamura, and K. Hono, Nat. Commun. **13**, 1817 (2022).
[29] E. Jurčišinová and M. Jurčišin, J. Magn. Magn. Mater. **572**, 170658 (2023).
[30] H. Kobayashi and M. Suzuki, Physica A **199**, 619 (1993).
[31] J. L. Monroe, J. Stat. Phys. **65**, 255 (1991).
[32] J. L. Monroe, J. Stat. Phys. **67**, 1185 (1992).
[33] J. L. Monroe, Physica A **256**, 217 (1998).
[34] M. Pretti, J. Stat. Phys. **111**, 993 (2003).
[35] E. Jurčišinová, M. Jurčišin, and A. Bobák, Phys. Lett. A **377**, 2712 (2013).
[36] E. Jurčišinová, M. Jurčišin, and A. Bobák, J. Stat. Phys. **154**, 1096 (2014).
[37] E. Jurčišinová and M. Jurčišin, Phys. Rev. E **89**, 032123 (2014).
[38] R. Liebmann, *Statistical Mechanics of Periodic Frustrated Ising Systems* (Springer-Verlag, Berlin, 1986), pp. 119–120.
[39] X. Yao, J. Magn. Magn. Mater. **322**, 959 (2010).
[40] E. Jurčišinová and M. Jurčišin, Physica A **521**, 330 (2019).
[41] E. Jurčišinová and M. Jurčišin, Phys. Lett. A **378**, 1059 (2014).
[42] E. Jurčišinová and M. Jurčišin, Physica A **461**, 554 (2016).
[43] E. Jurčišinová and M. Jurčišin, J. Magn. Magn. Mater. **451**, 137 (2018).
[44] E. Jurčišinová and M. Jurčišin, Physica A **561**, 125237 (2021).
[45] E. Jurčišinová and M. Jurčišin, Phys. Rev. E **104**, 044121 (2021).
[46] L. Pauling, J. Am. Chem. Soc. **57**, 2680 (1935).
[47] J. F. Nagle, J. Math. Phys. **7**, 1484 (1966).
[48] B. A. Berg, C. Muguruma, and Y. Okamoto, Phys. Rev. B **75**, 092202 (2007).
[49] R. R. P. Singh and J. Oitmaa, Phys. Rev. B **85**, 144414 (2012).
[50] P. D. Gujrati, Phys. Rev. Lett. **74**, 809 (1995).
[51] J. Ho-Ting-Hun and J. Oitmaa, J. Phys. A: Math. Gen. **8**, 1920 (1975).
[52] J. Adler, J. Phys. A: Math. Gen. **16**, 3585 (1983).
[53] R. J. Baxter, *Exactly Solved Models in Statistical Mechanics* (Academic Press, London, UK, 1982).
[54] A. L. Passos, D. F. de Albuquerque, and J. B. S. Filho, Physica A **450**, 541 (2016).
[55] K. Soldatov, K. Nefedev, Y. Komura, and Y. Okabe, Phys. Lett. A **381**, 707 (2017).
[56] E. Jurčišinová and M. Jurčišin, Physica A **554**, 124671 (2020).
[57] A. J. Garcia-Adeva and D. L. Huber, Phys. Rev. B **64**, 014418 (2001).
[58] J. G. Rau and M. J. P. Gingras, Nat. Commun. **7**, 12234 (2016).
[59] K. Mitsumoto, C. Hotta, and H. Yoshino, Phys. Rev. Res. **4**, 033157 (2022).